THE ASTROPHYSICAL JOURNAL

AN INTERNATIONAL REVIEW OF SPECTROSCOPY AND ASTRONOMICAL PHYSICS

VOLUME LXVI OCTOBER 1927 NUMBER 3

ON THE SPECTRUM OF HALLEY'S COMET

By N. T. BOBROVNIKOFF

ABSTRACT

The *spectrum* of the comet obtained with different instruments *was studied photometrically* and *compared with* the *direct photographs. The sizes and photographic density* of three monochromatic images of the head λ 3883 (*CN* IV), λ 4020–λ 4100 (*C*+*H*), and λ 4737 (*C* IV) were measured. The results indicate a *variation in size and brightness* of the spectral images of the comet as well as of the direct photographs in such a way that the large heliocentric distance favors more the development of the *CN* and *C*+*H* rather than the Swan bands. All *images* reached the *minimum size* about *one month after perihelion.*

Existence of *two types of continuous spectrum* in the comet was established. They are: the *solar type* with the maximum of intensity at λ 4700 due to the reflected sunlight and the *comet's own continuous spectrum* with the maximum at λ 4000, called the *violet type. Microphotometric records* obtained by means of a thermopile *show* an unmistakable *suppression* of the *violet type* spectrum and its consequent restoration *depending upon the heliocentric distance* of the comet. The change from one to the other type of the spectrum occurred at $r = 1.2$ astronomical units. When the comet was farther than this from the sun, the reflected sunlight did not contribute much to the brightness of the comet.

Frequent changes were observed in the spectrum of the comet with the corresponding changes on the direct photographs. Especially *notable* is the *suppression* of the *violet part* of the spectrum on May 23–24, 1910.

The distribution of intensity among the vibrational quanta of the Swan and cyanogen systems was found to *differ* considerably from the *laboratory data.* The shift of the intensity toward the higher quantum numbers was established in case of the Swan spectrum.

The structure of the head was studied in detail on the plates taken with the 60° prism and on the direct photographs. *An asymmetry* of the bands *was found.*

The spectrum of the jets and fine structure associated with the nucleus was isolated and studied. Cyanogen was found to play the predominant part in these phenomena. The spectrum of the condensation in the tail of the comet on June 7 was found to be gaseous, presumably belonging to CO^+.

Many papers have been published on this subject by various writers. The purpose of the present investigation is to study the development of the spectrum and the distribution of intensity among different bands of the cometary spectrum.

The material for this study consisted of fifty-three spectral plates (series OP) some of which have two images of the comet taken by J. A. Parkhurst with the ultra-violet Zeiss Doublet ($a = 14.5$ cm, $f = 81.4$ cm), the 15° objective prism having been used. The scale of these plates is 3.1 mm between $H\beta$ and $H\theta$. Another set of plates, only three of which were measurable, was obtained by O. J. Lee (series AP) with an objective prism of 60° and a small camera (Zeiss Anastigmat; $a = 7.1$ cm, $f = 44.9$ cm). The scale of these plates is about 27 mm between the same lines. In addition to this, many direct photographs of the comet obtained by E. E. Barnard with the Bruce telescope were measured and compared with the spectral images. Universal Time is used throughout this paper unless otherwise stated.

SPECTROPHOTOMETRIC INVESTIGATION

The changes in brightness of monochromatic images of the head and of the continuous spectrum of the comet were apparent at the first glance in such extensive series of plates as that of OP, covering more than six months (from December 19, 1909, to June 26, 1910). A systematic study of these changes was desirable in view of the total lack of information on the subject.

For precise measurement and comparison of the photographic densities of spectral images, many factors have to be eliminated. Of these the most important are: (1) difference in the exposure time; (2) difference in the development time; (3) chemical fog and effect of supplementary exposure; (4) atmospheric absorption. Other small factors were neglected after due consideration. The plates and developers used for this investigation were of the same, or of quite similar brands. The plates were Seed 27 and Lumière Sigma for the series OP and Cramer Isochromatic for the series AP. A self-registering thermopile microphotometer was used for this work, which introduced additional disturbing factors, such as absorption by the glass of the plate, absorption by the film, lack of uniformity of the silver grains. Experiments showed that the first factor was of very small importance as the glass was of nearly equal thickness. The absorption by the film was neglected, since it was small and not of systematic character and probably smoothed out in the long run.

The graininess of the plates produced frequent zigzags on the records; their effect, however, was negligible.

The difference in the exposure time and density of the fog on the plate was of fundamental importance in the measurement. In the cometary spectra obtained on ordinary plates two bands are of the greatest interest: Cyanogen λ 3883 and Swan λ 4737. They were denoted *CN* IV and *C* IV according to H. Kayser's notation.[1] Two filters approximately monochromatic for these wave-lengths were selected for the study of the blackening of the plate and its dependence on various parameters. They were Wratten light-filters of the Eastman Kodak Company: ultra-violet No. 18 for *CN* IV, and No. 75η for *C* IV.

A sensitometer with rotating sector was used for this study. The plate was illuminated by a lamp fed by a storage battery in a potentiometer circuit and screened by the above-mentioned filters. Thus a series of densities was obtained on the same plate, the time of exposure changing for each segment in a definite proportion. An additional lamp behind a white diffusing screen was established in such a way that its light fell on the exposed plate simultaneously with the monochromatic light, thus producing the fog on the plate. The current through this lamp was kept under close observation. By changing the intensity of this additional illumination a set of curves correlating the density of the silver deposit with the exposure time could be obtained for various combinations of the white and monochromatic illumination.

From these curves another set of curves could be easily deduced. They correlate the density of the fog on the plate and the true density of the image, that is, the density which would have resulted if the fog were not present at all.

The density D of the image measured on the plate is produced by the simultaneous action of the monochromatic light which would itself give a density d and by the supplementary exposure which produces the fog of the density δ. Now we have

$$d=f(\delta, D)\ ,$$

all other parameters being eliminated or being of small importance. It is evident that the curve of the density $D=a$ must intersect the

[1] *Handbuch der Spectroscopie*, **5**, 226, 1910.

ordinate d and the abscissa δ in the same point a. This locates the upper and the lower ends of the curve of the resultant density $D=a$. Several other points on this curve for the values of D, every 0.1 of the density scale, were found from the measurement of the sensitometer plates. These curves are given in Figures 1 and 2 for both filters. The lower parts of the curves are naturally less certain. The

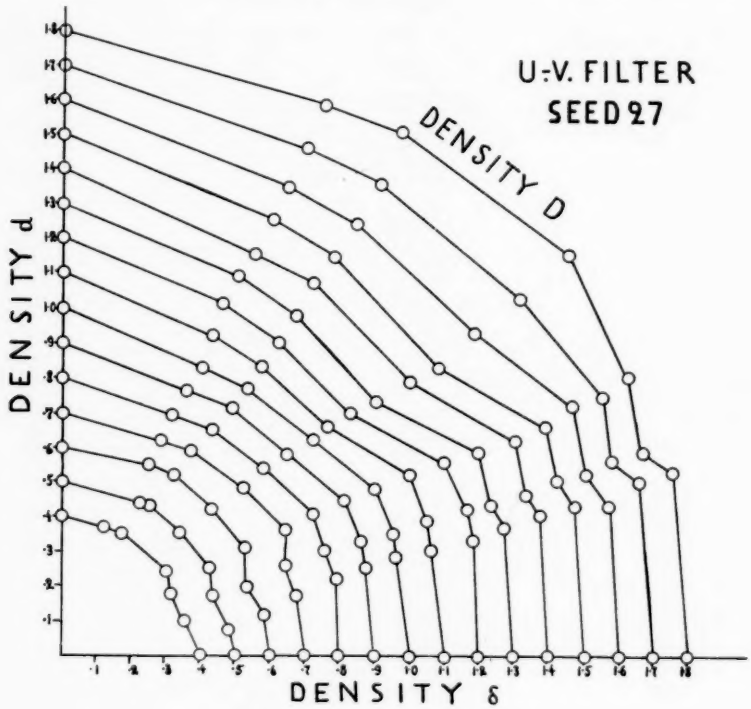

FIG. 1.—Curves for the elimination of fog

values found for the points of these curves are the means of many measurements from many plates and each curve in addition constitutes a good check on the adjacent curve. The complete series of experiments was carried out for Seed 27 plates only. The density d is obtained from these curves (Figs. 1 and 2) as the ordinate corresponding to the point of intersection of the line $\delta=a$ and the curve of the measured density D.

The time of development changes the slope, γ, of the straight

part of the characteristic curve very rapidly at the beginning and slowly when the time approaches full development. A set of curves for each filter for different times of development was derived from experiments. Fortunately the time of development did not differ

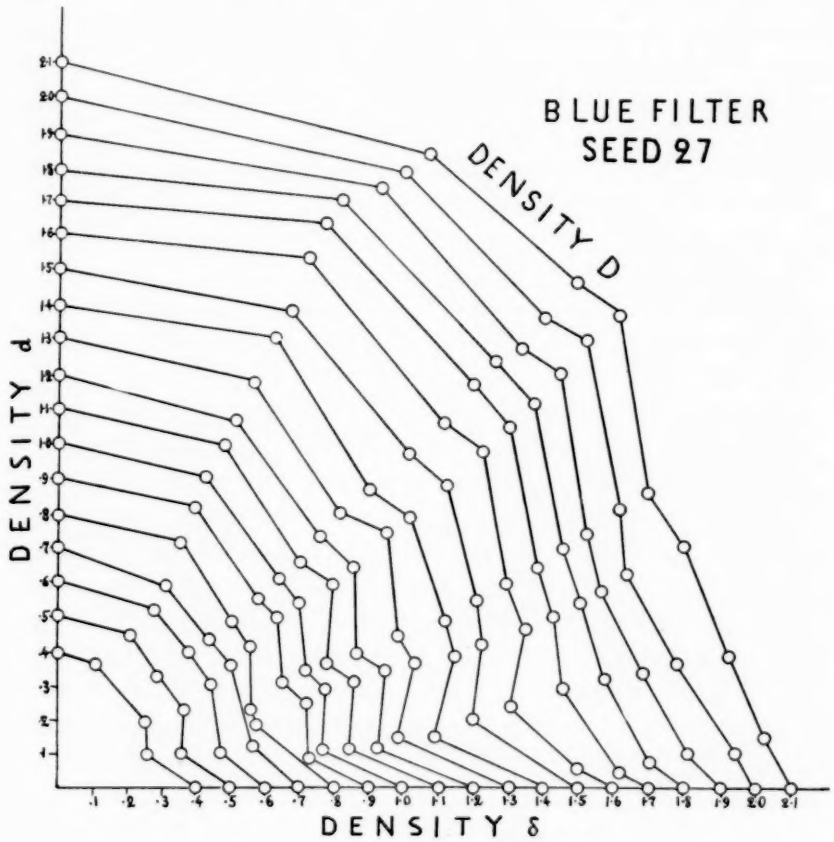

FIG. 2.—Curves for the elimination of fog

much in individual cases for the cometary plates and corrections were small.

The difference in exposure time was eliminated by means of the same set of curves. Knowing the logarithm of time corresponding on the graph to the density which we have to reduce (abscissa) and knowing the logarithm of the ratio between the standard and actual

time of exposure, we obtain the required density as the ordinate corresponding to the sum of these two logarithms.

Atmospheric absorption was reduced to standard conditions by means of comparison spectra of stars (usually of class A) which had been taken simultaneously with the spectrum of the comet. Densities of the continuous spectrum of such stars at the wave-lengths corresponding to the cometary knots were measured and reduced to an arbitrary standard condition. The correction was usually small.

The self-registering microphotometer used for this study consisted of a Coblenz thermopile (*Bi* and *Ag*, ten elements) and a Leeds and Northrup galvanometer. The deflections of the galvanometer were registered by means of an optical device on the photographic paper placed on a drum rotating in a simple connection with the plate under analysis. The deflections of the galvanometer were calibrated in terms of a photographic wedge of the Hartmann microphotometer. The wedge itself was calibrated in terms of photographic density by optical filters of neutral tint from the Eastman Kodak Company, transmitting a definite amount of light.

After some preliminary experiments the following order of reduction was adopted. The spectra were placed on the analyzing slit of the self-registering microphotometer before the thermopile and a record of their densities was thus obtained. On the same sheet of paper a photometric scale was impressed by means of which the maximum of the photographic density of the corresponding knots in the spectrum was determined. These densities were then reduced to a standard exposure and development time and the fog of the plate was eliminated. Finally, a correction for the changes in the atmosphere was applied. The densities then could be compared with each other.

The spectrophotometric method described above appears to be very laborious, but once the reduction curves have been obtained the rest is a simple matter. It was tested on many occasions with the plates having several spectral images of the comet with different exposure times. The agreement of the results was very satisfactory except for greatly overexposed images.

WAVE-LENGTHS

The measurement of the wave-lengths of the cometary radiations did not give essentially new results when compared with the thorough investigations by V. M. Slipher.[1] Measurements of plates taken with the 15° prism were reduced graphically, the wave-length of λ 3883 being assumed. The wire of the micrometer was set on the brightest part of the condensation representing the monochromatic image of the cometary head. The wave-length of the band *C* IV came out λ 4698±3.6, which means that the brightest band in this head was λ 4686 and not λ 4737. Each of the large-scale plates was reduced by the Hartmann-Cornu formula, the wave-lengths for three bands, λλ 3883, 4737, and 5635, being assumed. The prominent group of condensations between λ 4020 and λ 4108 were found to belong definitely to the combination $C+H$, discovered in the laboratory by Raffety.[2]

DIMENSIONS OF THE HEAD

The measurement of the diameter of the densest part of the spectral condensations was undertaken and proved to be quite feasible. The edges of this part of the condensation were sharp enough, and all settings were in good agreement unless the images were much over-exposed. The diameter perpendicular to the nuclear line of the spectrum was measured in all cases. It nearly coincided with the direction of the tail. Table I gives the results of these measurements. The diameter of condensations is given in thousands of kilometers. The effect of foreshortening was neglected in view of the probable spherical shape of the head. The second, third, and fourth columns give the sizes of the head in the bands *CN* IV, $C+H$, and *C* IV. The fifth column contains the diameter of the head of the comet across the nucleus, perpendicular to the axis of the tail on the direct photographs of the same date taken with the Bruce 10-inch telescope by Professor E. E. Barnard. The scale of the Bruce photographs is 161″ per millimeter, while for the OP plates it is 253″ per millimeter. The inner brighter envelope was measured on the direct photographs as

[1] *Lowell Observatory Bulletin*, No. 52.

[2] *Philosophical Magazine*, **32**, 556, 1916; also F. Baldet, *Comptes Rendus*, **177**, 1205, 1923.

explained above. The comparison of the dimensions of spectral images with the direct photographs shows at once that the latter were much larger and subject to greater variations as we might well expect. But the principal features of the changes undergone by the spectral images were followed faithfully by the direct images. This

TABLE I

SIZES OF THE IMAGES OF THE HEAD

DATE	OBJECTIVE PRISM			BRUCE 10-INCH	
	CN IV	*C*+*H*	*C* IV	Head	Halo
Dec. 18	71.9	49.6	49.5	.....	.....
Dec. 30	95.2	77.1	74.6	163.1	.....
Dec. 31	115.6	84.6	74.6	.....	.....
Jan. 9	135.0	64.9	97.0	154.9	.....
Jan. 15	90.0	64.5	84.5	178.2	.....
Feb. 4	65.2	42.0	57.7	222.5	.....
Feb. 10	62.5	42.8	69.0	230.6	.....
Mar. 8	69.1	.....	106.6	219.0	.....
Apr. 21	.....	.....	46.1	145.6	.....
May 4	21.2	8.0	40.5	115.3	.....
May 5	21.2	9.4	27.0	103.6	.....
May 7	16.5	.....	18.5	48.9	.....
May 21	.....	.....	5.9	.....	.....
May 24	2.8	3.8	8.5	39.6	77
May 25	5.8	5.3	7.3	81.5	191
May 26	16.0	10.8	12.3	97.8	221
May 27	15.4	9.4	14.3	97.8	185
May 28	14.5	14.5	14.7	101.3	261
May 30	27.0	26.3	46.0	138.6	.....
May 31	21.3	11.5	22.2	265.6	352
June 2	18.7	9.4	25.2	231.8	385
June 6	23.2	16.7	37.3	163.1	283
June 7	37.1	31.2	50.1	199.2	405
June 8	26.1	17.6	33.8	223.6	.....
June 10	27.2	23.9	35.1	111.8	.....
June 11	28.6	21.8	35.2	128.1	.....
June 12	24.2	19.9	23.3	.....	.....
June 13	42.2	25.8	51.5	116.5	.....
June 26	59.7	46.5	48.1	118.8	.....

correspondence is also good for the changes of spectral images and measurements of the nucleus on large-scale photographs by H. D. Curtis,[1] but values given by him are far too small in comparison even with the smallest *C*+*H* head on our spectrograms.

The last column of Table I gives the dimensions of the halo which is to be distinguished from the regular parabolic envelopes.

[1] *Publications of the Astronomical Society of the Pacific*, **22**, 117, 1910.

This halo appeared in the latter half of May, 1910, varying in size and brightness. Sometimes it was so bright as to obliterate the details of the envelopes (on May 28). Sometimes it was very faint in comparison with the envelopes (on May 30). In shape it was apparently a perfect sphere having the nucleus for its center. It made its first appearance on the plates of May 24, being very small and faint. The photographs of the beginning of May show no trace of it in spite of very bright envelopes. After June 7 it disappeared al-

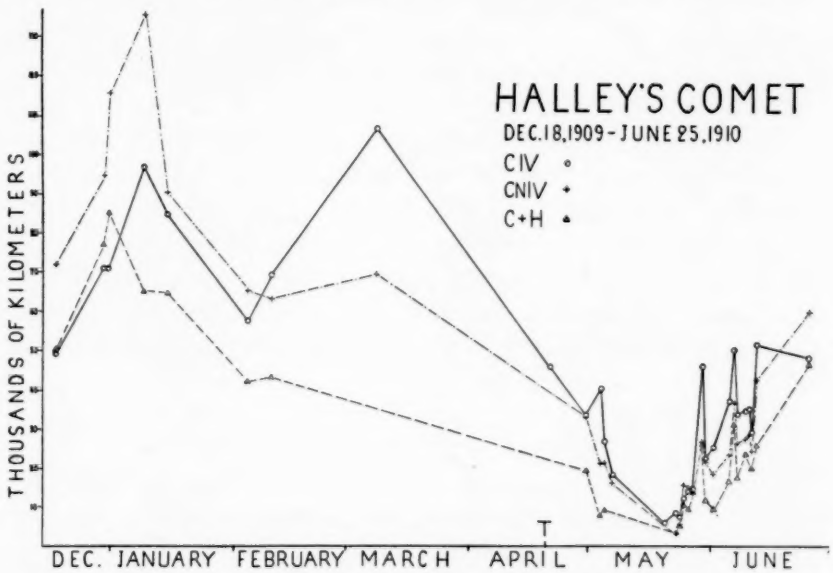

FIG. 3.—Size of spectral images in thousands of kilometers

together or became so small that it was masked by the envelopes. Possibly it developed in connection with the violent changes in the head of the comet on May 23–24, as we shall see later.

This halo was measured on the Bruce plates taken with the 10-inch lens. In view of its faintness in comparison with the head no spectral image of it could be obtained except on Plate AP_5, taken on May 27.

Figure 3 represents the variation in size of different heads in the spectrum.

The diminution of the heads with the approach to perihelion and

subsequent increase is apparent. All spectral images and the direct image of the head as well as the nucleus on the direct photographs (by H. D. Curtis) attain their minimum size not exactly at perihelion, denoted on the graph by letter T, but one month later somewhere around May 24. There must have been a lag in the development of activity with the comet's position with reference to the sun.

In view of the difficulty of measurement it is impossible to insist on the reality of the frequent and irregular changes in the dimensions of the head. Some of them, at least, must be real. The direct photographs show quite similar changes following the spectral images closely. There seems to be an indication of periodicity in the ascending branch of the curve.

An important distinction in the way of variation of the head *CN* IV and *C* IV is evident. When the comet was far from the sun *CN* IV was much larger than *C* IV. They became of equal size at the beginning of February and after that *C* IV was considerably larger. In the middle of June the reverse took place. The $C+H$ knot behaved like *CN* IV but its dimensions were always smaller than those of *CN* IV. It became smaller than *C* IV at an earlier date and became equal again to *C* IV later than *CN* IV.

BRIGHTNESS OF THE SPECTRAL IMAGES

The density of the spectral images in *CN* IV, $C+H$, and *C* IV was measured. It was reduced to a standard exposure time of ten minutes and to full development, and fog was eliminated as was explained above. For the reduction to the standard atmospheric conditions for which those of May 26, OP314, were adopted, Regulus was used. For the dates earlier than May 5 the conditions of OP290, May 5, were taken as standard. Both dates were described by Parkhurst in the same words in the *Journal of Observations* as to the conditions of transparency and seeing. The altitude of the comet was almost identical, so that the discrepancy between these two sets of observations cannot be large. The plates before March 9 and after June 12 were not corrected because of the absence of a comparison spectrum. From the description of atmospheric conditions, no large correction could be expected. The value of OP289, April 30, also was not corrected and probably should read somewhat higher. Table II gives

the results. Values in parentheses are not certain for various reasons. The discrepancy of values for May 24 is explained by a sudden

TABLE II

PHOTOGRAPHIC DENSITY OF SPECTRAL IMAGES

No. OP	Date	*CN* IV		*C*+*H*		*C* IV	
245	Dec. 20.3	0.20		.....		0.01	
246	Dec. 30.0	.32		.....		.14	
247	Dec. 31.1	.28		.....		.01	
248	Jan. 4.1	.43		0.41		.04	
250	Jan. 9.1	.37		.....		.22	
251	Jan. 15.1	.20		.....		.08	
261	Feb. 4.1	.37		.23		.23	
265	Feb. 10.1	.20		.....		.08	
269	Feb. 28.1	.10		.07		.20	
272	Mar. 8.1	(.01)		.....		.02	
287	Apr. 21.4	(.60)				.80	
289	Apr. 30.4	.62		.35		.56	
290	May 4.4	.37	0.54	.33	0.44	0.72	0.99
291	May 4.4	.70		.54		1.26	
294	May 5.4	0.93		.82		1.37	
295	May 7.4	1.00		0.99		1.20	
296	May 10.4	(0.50)		.....		0.70	
305	May 21.1	(0.70)				0.90	
306	May 24.1	1.48		1.48		1.93	
307	May 24.1	1.38	0.95		1.15	2.03	1.65
308	May 24.1	0.58		0.83		1.42	
309	May 24.1	0.34				1.23	
311	May 25.1	.....		.....		1.23	1.48
312	May 25.1	1.27		1.54		1.73	
314	May 26.1	1.25		1.37		1.88	
318	May 27.2	1.20		1.30		1.73	
319	May 28.2	0.77	0.75	0.85	0.80	0.70	1.00
320	May 28.2	0.73		0.76		1.30	
321	May 30.1	1.06		1.06		1.45	
322	May 30.1	0.98		0.91		1.35	
324	June 2.1	1.37		1.37		1.60	
326A	June 6.1	1.24	1.30	1.24	1.30	1.37	1.40
326B	June 6.1	1.37		1.37		1.43	
327A	June 7.1	1.35	1.15	1.35		1.45	1.25
327B	June 7.1	0.95				1.05	
328	June 8.1	.83		0.79		0.87	
329	June 10.1	.43		.43		.92	
330	June 11.1	.67		.57		.88	
331	June 12.1	.51	0.43	.49	0.38	.50	0.42
332	June 12.1	.35		.27		.35	
333	June 13.1	.52		.51		.40	
334	June 15.1	.24		.22		.10	
335	June 26.1	0.10		0.10		0.04	

change in the head of the comet as we shall presently see. The average uncertainty of the whole series is estimated at 20 per cent of the given value.

Figure 4 is the graph constructed from this table for the knots *CN* IV and *C* IV.

The ordinate gives the logarithm of intensity of the corresponding heads. Really it is the photographic density reduced to the same

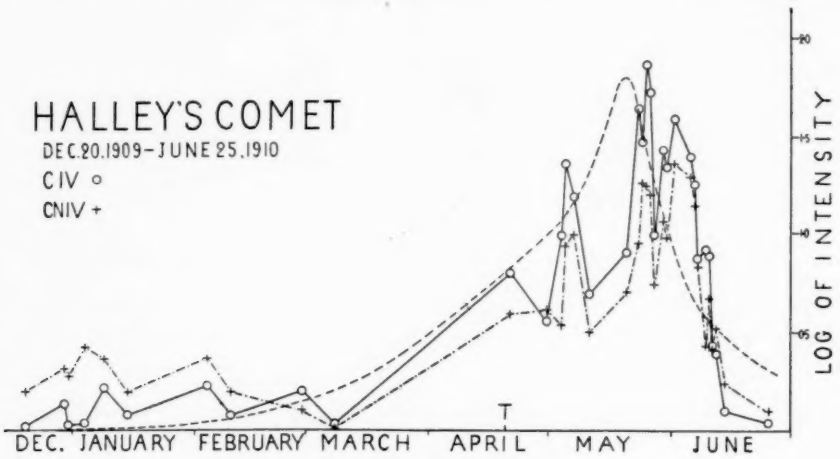

FIG. 4.—Intensity of spectral images

time of exposure t. The photographic density, however, can be approximately expressed through the relation

$$d=\log It^{p}-i\,,$$

where I is the intensity of light and p and i are constants. We have for two densities d_1 and d_0

$$d_1-d_0=\log\frac{I_1}{I_0}\,,$$

if t is the same throughout the whole series of the plates as in our case. Therefore the ordinate is proportional to the logarithm of intensity. For λ 3883 (*CN* IV) and λ 4737 (*C* IV) γ is different so that the two curves should have different ordinates. Since, however, the difference is not large and since we are interested more in the general character of the curves than in the absolute values of intensity, no attempt was made to reduce both curves to the same ordinate. The first five plates are Sigma, whereas the rest are Seed 27. This results in a slight raising of the curves at the beginning because of the great-

er sensitivity of Sigma plates. But the general character of the distribution of intensity between the knots *CN* IV and *C* IV could not be changed by this fact, as it is clear from the records of stellar spectra on both of these plates.

Each monochromatic image of the head consists of the radiations of the head and the continuous spectrum at that place. The continuous spectrum of the comet consists of the reflected sunlight and the light of the comet itself. That part of it which belongs to the reflected sunlight should vary according to the law

$$I=\frac{I_0}{r^2\Delta^2},$$

$$\log I=\log I_0-2\log r-2\log\Delta.$$

Owing to the small scale and small dispersion of the spectrograms the effect of intercepting the analyzing beam of light in the thermopile and consequently the deviation of the galvanometer should be ascribed to the total brightness of the comet or blackening due to it, and not to the surface brightness to which it would be ascribed in the case of large-scale photographs.

The smooth curve was drawn according to the above-mentioned formula and was so placed as to coincide with the first date of the investigation on the x-axis. The constant I_0 was chosen to fit observations the best. The correction in phase was neglected in view of uncertainty on this question.

Examination of Figure 4 reveals interesting features of the spectral variations. However we may shift the theoretical curve in the ordinate, it is clear that the changes in the brightness of the spectral images follow in general the curve. The reflected sunlight constituted a considerable part of the total light of the head near the perihelion passage. The frequent variations in intensity are far too large to be explained by the errors of measurement. The curve of visual brightness of both the nucleus and the head of the comet exhibits similar deviations from the smooth line. The maximum of the curves obtained is shifted to the right for about a week or two in comparison with the theoretical maximum. This may be compared with the similar lag in the development of the head as we have seen in the case of

the size of spectral images. The abnormally rapid decrease in brightness in the descending branch of the curve is in agreement with the photometric study by A. Bemporad.[1] It means a larger exponent for r in the well-known expression $I = I_0/r^n\Delta^2$, and, indeed, the first part of the curves is better satisfied with $n = 2$, while the second with $n = 4$.

It is evident from the graph that the intrinsic light of the comet favors more the violet side of the spectrum than the blue. *CN* IV was considerably brighter than *C* IV at the beginning of observation. They became of equal brightness by the middle of February after which time *C* IV was much brighter than *CN* IV. Combining this result with the result of the measurement of the size of the spectral heads, we may say that when the comet was far from the sun the *CN* IV head was larger and brighter than the *C* IV head with consequent reversal of this relation at the approach to perihelion and its restoration when the comet was again far from the sun. The *C*+*H* head behaved very much like *CN* IV. It should be borne in mind that the established relations concern the brightness of different heads as they are recorded on the blue-sensitive plates. Taking into account the low sensitivity of the ordinary plates to the violet compared to the blue light, we may expect the curve *CN* IV to be shifted along the ordinate, but, of course, whatever has been said of the general character of the changes remains true. It seems that the large heliocentric distance is more propitious for the development of the violet side of the spectrum than of the blue. The amount of the reflected light in the comet at the beginning of the year 1910 was so minute that the total luminosity of the comet should be ascribed to the inherent light. In May the comet shone principally by the reflected light which favors the brightness of the *C* IV band. An estimate of the ratio of the brightness of the reflected light at its fullest development in May to the inherent light in December is 15:1.

The rapid changes that were going on in the comet are beyond doubt. Especially the sudden increase in brightness on May 4–6 should be noted. The data are too meager for us to draw any conclusions on the periodic variations in brightness, though their possibility cannot be denied. Between May 10 and 20 there were prob-

[1] *Memorie della Società degli Spettroscopisti italiani*, **40**, 163, 1911.

ably some more variations in light that would bring the curve to a better correspondence with the theoretical curve at that place.

DEVELOPMENT OF THE SPECTRUM

If we turn now to the study of the variation of the spectrum of the comet as recorded by the thermopile microphotometer, we shall find further corroboration of the existence of two distinct types of the continuous spectrum in this comet: the solar type with the maximum of intensity at λ 4700, and the comet's proper spectrum with the corresponding maximum at λ 4000.

Figure 5 shows the spectrum of the comet taken at two characteristic dates, together with the spectrum of Capella, which for this

TABLE III

DEVELOPMENT OF THE SPECTRUM

No.	Series OP	Date	Exposure	Plate	r
1.....	245	Dec. 19, 1909	125^m	Sigma	2.18
2.....	261	Feb. 3, 1910	31	Seed 27	1.55
3.....	265	Feb. 9, 1910	60	Seed 27	1.46
4.....	269	Feb. 27, 1910	60	Seed 27	1.17
5.....	272	Mar. 7, 1910	30	Seed 27	1.06
6.....	289	Apr. 20, 1910	11	Seed 27	0.64
7.....	294	May 6, 1910	5	Seed 27	.67
8.....	306	May 23, 1910	5	Seed 27	0.91
9.....	321	May 29, 1910	10	Seed 27	1.01
10.....	332	June 11, 1910	27	Seed 27	1.22

purpose may represent the solar spectrum. The continuous spectrum is approximately traced by broken lines. It is clear that on May 6, 1910, the cometary continuous spectrum followed the solar spectrum very closely. On the contrary, on January 14, 1910, the continuous spectrum was altogether different from the solar. The first type of the cometary continuous spectrum we shall call the "solar-type spectrum," the other the "violet-type spectrum."

Ten plates were selected from the whole collection to illustrate the development of the spectrum of the comet. The necessary data are given in Table III; the time is Central Standard Time.

We see from Figure 5 that in December the comet's light consisted chiefly of the continuous spectrum of the violet type, the bands being hardly noticeable. They developed, however, very soon. On

February 3 the comet still had its characteristic continuous spectrum with bands already highly developed.

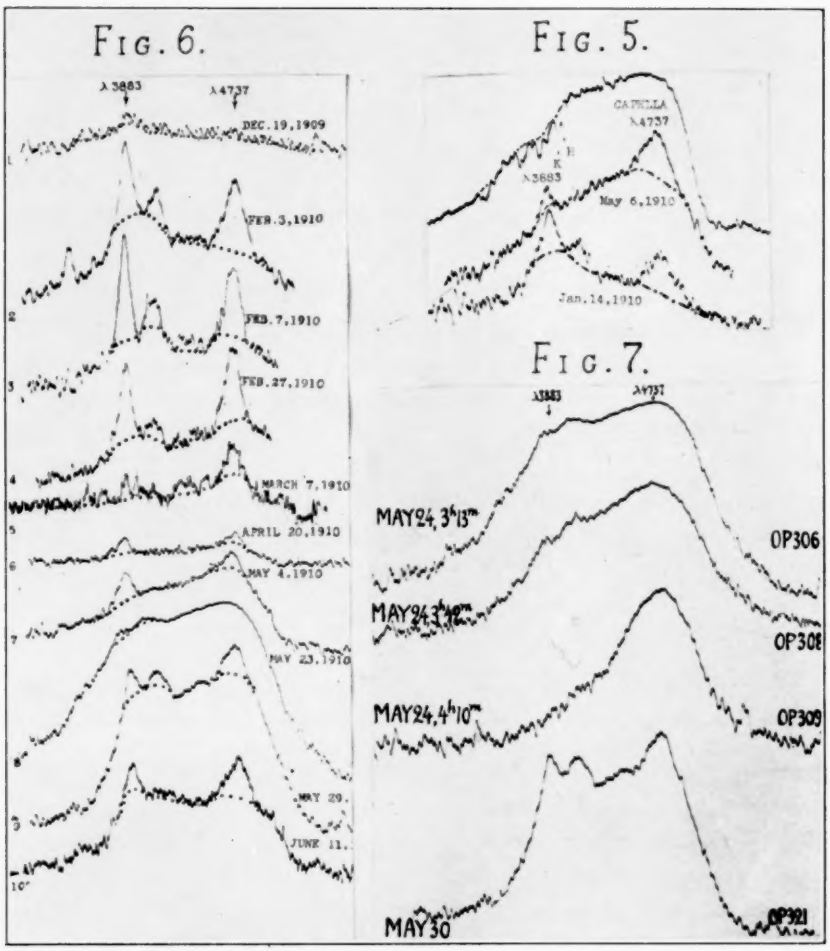

FIG. 5.—Spectrum of Halley's comet
FIG. 6.—The development of the continuous spectrum of Halley's comet
FIG. 7.—Changes in the head of the comet on May 24, 1910

The reflected solar spectrum makes its first unmistakable appearance at about the middle of February. At the end of this month the solar spectrum is already stronger than the violet and in April and May it is the predominant feature of the whole spectrum. On May

29 the first signs of the violet spectrum reappear and on June 11 the maximum of intensity of the continuous spectrum is in the violet, resembling thus the condition on February 3. This is in contradiction with the general but unwarranted opinion that when the comets are far from the sun they shine chiefly by the reflected sunlight.

The continuous spectrum in Figure 6 is indicated by the dotted line. While in some cases its course may be questioned, no doubt can be maintained as to the development just described. Both changes from and to the violet-type spectrum occurred at nearly the same heliocentric distance (1.2).

The question which suggests itself in the use of a self-registering microphotometer in a case like ours is how far the curves of intensity can be trusted. Is it really a continuous spectrum or simply faint radiations that cannot be separated by the instrument? Especially in the case of the bands of *CN* IV and *C*+*H* there may arise a suspicion of overlapping. A little consideration convinces us that there is no such danger. The thermopile in the arrangement used for this work could readily separate the lines which are 0.15 mm distant. On the OP plates the edges of the bands *CN* IV and *C*+*H* were usually 0.60 mm distant. Furthermore, the spectra of other comets taken with the 30° and 15°+30° prisms, where there is no question of overlapping, show the same continuous spectrum as do the plates obtained with the 15° prism. The same is true of the 60° prism. The great regularity of the run of the continuous spectrum is in itself a good criterion.

It is an interesting question whether these changes were caused by the gradual dying out of the violet continuous spectrum and *CN* band with the approach of the comet to the sun or because they seemed faint in comparison with the brightness of the reflected solar spectrum. It is impossible to decide this in view of the great complexity of the cometary phenomena, but evidence points rather to the latter conclusion, namely, that the decrease in brightness of *CN* and, therefore probably of the violet-type continuous spectrum, was only apparent. Taking into consideration the difference between the density of the bands and their continuous background, we are forced to the conclusion that *CN* IV and *C*+*H* bands increase in brightness with the comet's approach to the sun, while *C* IV does not increase so

much and even sometimes altogether vanishes on the continuous background. The principal part in the spectral variations was apparently played by the continuous spectrum of both types.

SUDDEN CHANGES IN THE COMET

Apart from the gradual development of the spectrum there were many sudden changes in this comet, the most remarkable of which happened on May 24. Table IV supplies the necessary data for the spectrograms, as well as for the direct photographs taken with the Bruce 10-inch lens on the same date.

TABLE IV

CHANGES IN THE HEAD OF THE COMET ON MAY 24, 1910

No. OP	Date	Objective-Prism Plates					Direct Photographs		
		Mid-Exp.	Exp. T	Object	Density		No.	Mid-Exp.	Exp. T
					C IV	CN IV			
306.. .	May 24	3^h13^m	5^m	Comet	1.93	1.48	311	3^h10^m	19^m
307....	May 24	3 23	5	Comet	2.03	1.38	.....	.....	.....
308....	May 24	3 42	10	Comet	1.42	0.58	312	3 36	17
309....	May 24	4 10	10	Comet	1.23	.34	313	4 09	24
309....	May 24	4 15	.....	Regulus	.....	.....	.....	.....	.....
321....	May 30	4 01	10	Comet	0.92	0.68	.....	.....	.....
321....	May 30	4 06	.....	Regulus	.....	.....	.....	.....	.....

As it may be seen from Figure 7 there was on that night a gradual disappearance of the violet part of the spectrum with a corresponding, but not so marked, weakening of the rest of the spectrum. The curve from OP306 shows a well-developed spectrum with the CN IV and $C+H$ bands. The next curve corresponding to an exposure only twenty-nine minutes later shows a considerable decrease in intensity of the violet part of the spectrum. On the plate OP309 twenty-eight minutes later still no trace of CN IV is left and but a faint trace of $C+H$. The measurement of intensity shows that C IV also underwent a considerable weakening, but not with so striking an effect. For comparison, an intensity curve from OP321, May 30, is given. It shows the normal development of the violet part of the spectrum. Any possibility of atmospheric or instrumental changes is

excluded, as the comparison spectra of Regulus on both dates give identical curves of intensity.

The direct photographs obtained by Barnard almost simultaneously with the corresponding spectrograms show a gradual swelling up of the nucleus. On the plate 311*a* at 3^h10^m the nucleus is rather large, spherical, about 40″ in diameter, with two attached wings which are less bright than the nucleus, but brighter than the rest of the head. They are symmetrical with respect to the axis of the tail. This corresponds to the spectrum of OP306. On the plate 312*a*, at $3^h\ 36^m$, the nucleus looks like an equilateral triangle whose vertex is on the axis of the tail pointed toward the sun and the two sides symmetrically situated with respect to the same axis. Each side of the triangle is about 90″. One corner is brighter than the rest, the diameter of the brighter part being 65″. This description corresponds to the beginning of extinction of the violet part of the spectrum. On the plate 313*a*, at 4^h9^m, the nucleus has the shape of an ellipse with the major axis of 130″ and the minor of 70″. This is the last stage of the extinction of the violet part of the spectrum.

Apparently this was not the end of the phenomenon. H. D. Curtis[1] describes an explosion in the nucleus almost coinciding in time with the Yerkes plates. His first picture, exposure 1^m, was taken with the Crossley reflector of the Lick Observatory at 4^h19^m, May 24, that is, at the end of the exposure of the Yerkes plate 313*a*. The diameter of the densest part of the condensation around the nucleus is given by Curtis as 3″. His next plate exposed from 6^h17^m to 6^h19^m shows very bright growths, roughly spherical, formed on each side of the nucleus. Their diameter was 37″. Under some assumptions the velocity of the masses at the explosion was found of the order of 1 km/sec.

In connection with the explosion just described may be the appearance of a straight jet or horn on the plates 311*a* and 311*b* making an angle with the direction of the tail of about 15°. It is quite distinct from the wings attached to the nucleus forming the head of the inner envelope. This jet is easily noticeable on the plate OP307. Its spectrum consists of monochromatic emissions of *CN* IV, *C*+*H*, *CN*

[1] *Op. cit.*, **22**, 121, 1910.

II (λ 4706), and *C* IV. The brightest jet is formed by the *CN* IV band in spite of its weakness in the head comparing with *C* IV, which is quite natural, taking into account that the brightness of the *C* IV band is much influenced by the solar continuous spectrum. It should be noticed that *CN* II is also present in the jet; although much brighter in the head, *CN* III (λ 4216) is absent. It is impossible to say anything definite about the continuous spectrum of the jet in view of the strong spectrum of the tail. It appears that this jet gave only a bright gaseous spectrum without any continuous background. The same jet may be noticed on the spectral plates OP306 and OP308, but not of such intensity.

Seven hours before the first Yerkes photograph was taken apparently similar jets were observed visually by K. Graff[1] at Bergedorf. To this must be added the development of the halo first noticeable on the Yerkes plates of this date.

On the next night, May 25, the head of the comet on the plates 315*a* and 317*a* has a peculiar outlook. It seems to have two envelopes, one narrow in the usual position in respect to the nucleus, the other much broader with the axis displaced and not so much extended toward the sun, as if it had its own invisible nucleus. Indeed, the secondary nucleus was observed on this date by W. F. Gale.[2] On May 26, at 10^h the head was photographed by C. P. Butler[3] with two distinct nuclei.

We can sum up the whole development of this remarkable phenomenon as follows:

May 23,	20^h.	Many jets around the nucleus (Graff).
May 24,	3^h13^m.	Nucleus rather large; spectrum usual; bright steady jet.
	3^h42^m.	Nucleus still larger; violet part of the spectrum weak.
	4^h10^m.	Nucleus very much larger; appendages; extinction of the violet part of the spectrum; faint halo.
	6^h18^m.	Two globular growths on both sides of the nucleus (Curtis).
May 25.		Double nucleus and two systems of envelopes; halo brighter.
May 26.		Nucleus double; halo much brighter.

All these striking transformations may be described as an explosion of the nucleus. The envelopes of gases formed at this ex-

[1] *Mitteilungen der Hamburger Sternwarte*, **5**, 62, 1913.

[2] Quoted by P. Stroobant, *Annuaire Belgique*, p. 362, 1912.

[3] *Proceedings of the Royal Society of London*, A, **84**, 523, 1910.

plosion intercepted the light of the nucleus, affecting chiefly the violet and ultra-violet part of the spectrum. This may indicate that their principal constituent was *CN*. These gases, inactive at the explosion, were soon activated by the sun's rays with consequent restoration of the usual spectrum. It is possible that in connection with this is the halo which lasted until the beginning of June.

It may be said that the spectral images of the comet's head were never exactly the same even on the plates taken immediately one after another, just as on the direct photographs. The jets and prominences are noticeable on many plates, especially on OP294 (May 5), OP318 (May 27), OP324 (June 2), and OP328 (June 8). The plate of June 8 is especially remarkable for the spiral structure of the head. All these jets and spirals can be identified on the direct photographs.

The *CN* IV band played apparently the most important rôle in the ejections.

STRUCTURE OF THE HEAD

The spectrum of the comet on the plate AP5, May 27, was selected for the detailed study of the cometary head. It is typical for the comet in the second half of May.

The tail made an angle of 20° with the line of the continuous spectrum on the plate. Owing to the peculiar shape of the central part of the head such position of the tail gave sharp edges to the bands in the spectrum, resembling those obtained with the slit spectrographs.

The continuous spectrum is a fine thread barely measurable. It is from 5″ to 6″ in breadth, the scale being 488″ to 1 mm and 217 km to 1″. The condensations are not symmetrical with respect to the nuclear line. The side on which the tail is situated is indicated by *t*, the opposite side by *s*. Table V gives the width of bands with estimated intensities on the scale of 10 for the brightest band and 1 for a band barely visible. No attempt was made to allow for the minimum sensitivity of the isochromatic plate in the green.

The head of the comet was measured also on the plate 331*a* taken almost simultaneously with the 10-inch Bruce telescope with an exposure from 2^h24^m to 3^h23^m. The head consisted of: (1) a nucleus small and round, of a diameter 5″.8; (2) two wings, *a* and *b*, attached to the nucleus (Fig. 7) approximately of the same size, the wing *b*

being much brighter. A circle having the nucleus for its center and a radius equal to 190″ would include both wings. Their common boundary was sharply defined and almost coincided with the axis of the tail. The flank edges of the wings coincided with the outline of the inner envelope and were apparently of parabolic shape. Their rear boundary was a sharp curved line; (3) an outer envelope of

TABLE V

WIDTHS OF INTENSITIES OF BANDS

Band	λ	*i*	*t*	*s*	Total
C II-1	5635	8	123	41″	164″
C II-2	5573	9	137	55	192
C II-3	5548	10	156	69	225
C II-4	5504	9	124	32	156
C II-5	5489	9	106	23	129
C III-1	5171	5	100	60	160
C III-2	5146	6	105	69	174
C III-3	5103	5	55	37	92
C III-4	5077	4	50	32	82
C IV-1	4737	6	69	37	106
C IV-2	4717	7	87	46	133
C IV-3	4696	8	110	73	183
C IV-4	4687	7	101	60	161
C IV-5	4681	5	64	46	110
CN II-1	4607	5	64	46	110
CN II-2	4585	4	55	32	87
CN II-3	4571	3	52	30	82
C+*H*	4313	3	.....	.....	5″–10″
C V-1	4382	3	27	50	77
C V-2	4372	4	28	18	46
C V-3	4365	2	25	16	41
CN III-1	4216	4	14	41	55
C+*H*	4075–4020	3–4	27	69	96
CN IV-1	3883	8	92	87	179
CN IV-2	3870	6	37	83	120
CN IV-3	3862	5	14	78	92

approximately parabolic shape, not so bright as the inner one. Its diameter through the nucleus perpendicular to the axis of the tail was about 600″; (4) a halo perfectly spherical in shape with the nucleus for its center, of diameter 800.″

If we compare now these results with the spectrum it becomes clear that the continuous spectrum was due to the nucleus proper which has the same width. The sharply defined wings gave rise to the band spectrum of *CN* and Swan as follows from the shape of the images and the dimensions of the wings. The outer envelope is also

present in the bands and the halo around the *CN* IV band is faintly visible. It is of the same size as on the direct photograph. Whether the halo is produced by other bands cannot be decided because of the tail which might mask it. A very faint continuous spectrum of the envelopes can also be traced. On the diagram of the spectrum (Fig. 8) the vertical scale is about twice the horizontal.

The dimensions of the $C+H$ knots and any other knot show that they were not purely nuclear emissions. The nucleus proper emitted all bands which are present in the head, because all bands become enhanced when they intersect the continuous spectrum. The inner brighter envelope consisted of radiations *CN* and Swan, which is probably also true of the outer envelope. We have seen that the

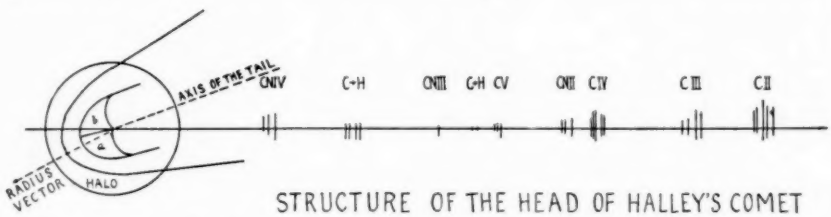

FIG. 8.—Structure of the head of Halley's comet

jets have the same composition. No electrical theory of the formation of the cometary envelopes can yet account for the fact that they consist of neutral molecules of *CN* and C_2H_2 if we accept the latter as the emitter of the Swan bands.

Greater brightness of the upper wing (Fig. 8) explains the asymmetry of most heads in respect to the nuclear line. However, it does not explain why some of the bands have their lower part longer.

RELATIONS OF INTENSITY

Tables VI and VII give the estimated intensities of the cyanogen and Swan bands in the usual scheme of the quantum theory, n' being the initial and n'' the final vibrational quantum numbers. In the normal case of the distribution of intensity the $0\rightarrow 0$ band should be the brightest, as well as any head in the sequence. The sequence $n'\rightarrow n''=0$ should be in a trough, and the maximum of intensity should run in a parabola from the $0\rightarrow 0$ band.[1] If we compare

[1] *Molecular Spectra in Gases, Bulletin 57, National Research Council*, pp. 121 ff., 1927.

Tables VI and VII with the laboratory intensities[1] we shall find at once considerable difference. The band of the maximum intensity is not the first in the sequence for the Swan spectrum; it is the second or even sometimes the third. In the case of cyanogen no trough is present. The properties of the photographic plate have nothing to do with this, since the whole sequence occupies a small part of the spectrum and different sequences show the same effect. All plates examined of series AP gave the same results, as well as the single

INTENSITIES OF BANDS

CYANOGEN

TABLE VI

n' \ n''	0	1	2	3	4	5
0	8	4	5			
1		6	3	3		
2			5	2		
3				3	1	
4					(1)	(1)
Sequence					CN IV	CN III

SWAN

TABLE VII

n' \ n''	0	1	2	3	4	5	6
0	5	8					
1	6	6	9				
2	3	7	5	10			
3		4	8	4	9		
4			2	7	(3)	8	
5				(1)	4		8
Sequence				C V	C IV	C III	C II

measurable plate IB²2349, May 24, taken with the Bruce spectrograph and 40-inch refractor by Professor E. B. Frost. This also accounts for the fact that the wave-length for the C IV band on the OP plates was found to be λ 4698, the brightest part of the head on which the wire of the micrometer was set. It is important to notice that the brightness of the band and its dimensions usually go together, that is, the brighter the band the longer it is. The beadlike shape of the cometary heads on the spectrograms of sufficient dispersion is, indeed, a characteristic feature. This would not be the case if the first band of the sequence were brighter and longer. The shift of the intensity toward the higher quantum numbers in the sequence $n' \rightarrow n'' = \text{const.}$ together with the relative abundance of the

[1] Given for the Swan spectrum by R. C. Johnson, *Philosophical Transactions of the Royal Society of London*, A, **226**, 157, 1927.

PLATE V

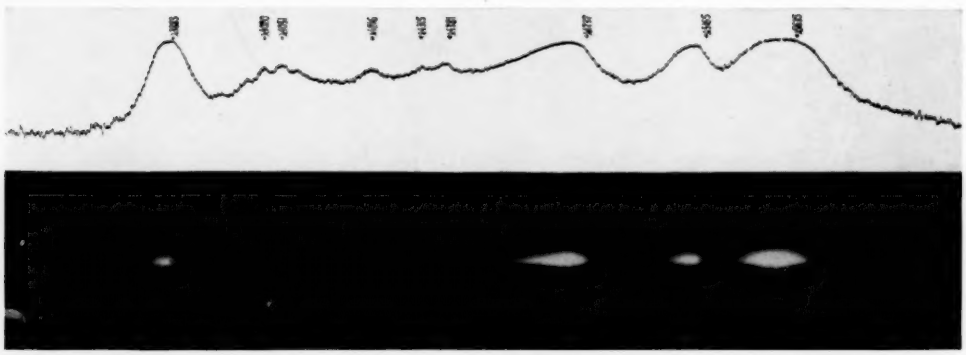

SPECTRUM OF HALLEY'S COMET, MAY 27, 1910
Exposure from 2^h46^m to $4^h\ 29^m$ U.T.

molecules in different states of transition seems to indicate that this is not the case of the thermodynamical equilibrium.

Plate V represents the spectrogram AP5 discussed in this section and its intensity curve. The shift of the intensity mentioned above is evident. The starlike appearance of the band λ 4315 $(C+H)$ is well pronounced.

Although many OP plates have images of the tail, the dispersion is insufficient to allow any investigation. On the plate OP327, June 7, the well-known condensation[1] moving outward is easily seen. All details of the direct photographs are reproduced on this spectrogram. The sharp edge of the condensation on the violet side similar to that of the tail streamers seems to indicate that the condensation was of the same gaseous character as the streamers, that is, consisted of CO^+.

PREVIOUS APPARITIONS

It is interesting to note that many phenomena associated with Halley's comet are apparently connected with its internal structure and repeat themselves in various apparitions of the comet.

It was most thoroughly observed in 1835 by Bessel[2] and others. Bessel describes it as an exceedingly changeable object. His drawing of the head of the comet of October 22, 1835, with the wings attached to the nucleus is almost identical with the Yerkes photograph of May 27, 1910, discussed above, even in the dimensions of the wings. His drawings suggest also the existence of a halo, but he never mentions it explicitly. The halo appearing and disappearing suddenly was observed by Maclear[3] in 1835 and 1836 at the Cape of Good Hope. The ejections from the nucleus were frequently observed by Bessel. Bright jets associated with the nucleus were seen[4] by Hevelius in 1682 and by many observers in 1759.

YERKES OBSERVATORY
July 1927

[1] Barnard, *Astrophysical Journal*, **39**, 379, 1914.

[2] *Abhandlungen von F. W. Bessel*, **1**, 54–80, 1875.

[3] *Memoirs of the Royal Astronomical Society*, **10**, 92, 1837.

[4] A. C. D. Cromellin, "Comets," *Splendour of the Heavens*, 1923, p. 393.

ON THE RADIAL VELOCITY AND SPECTRUM OF THE CEPHEID VARIABLE T MONOCEROTIS[1]

By ROSCOE F. SANFORD

ABSTRACT

Light-Curve.—The discovery and subsequent photometric observation of T Monocerotis are briefly discussed, and reasons are adduced for accepting the type of regular light-variation displayed by Wendell's curve, which has the maximum 5.61 mag., the minimum 6.77 mag., and an interval of seven days from minimum to maximum light. The maxima over the interval from 1874 to the present are best represented by

$$\text{Max} = \text{J.D. } 2410012.1956 + 27.003131E + 0.000025221E^2, \text{ G.M.T.}$$

which is Bemporad's formula with a somewhat larger value of the coefficient of E^2.

Radial-velocity curves.—Fifty values of radial velocity have been used to derive the general radial-velocity curve. Three of these were obtained by Frost at the Yerkes Observatory in 1905 and the remainder at Mount Wilson between 1917 and 1927 (Table II). The foregoing formula was found to be best suited to grouping all the radial velocities into a single cycle, and was used to derive the velocity-curve (top of Fig. 1).

Coincidence of maximum light and minimum velocity, and minimum light and maximum velocity, are brought out. Two contrasts between light-curve and velocity-curve are noted, one being the inflection in the latter about ten days after minimum velocity with no counterpart in the best light-curves, and the other, the blunt maximum of the velocity-curve as compared with the rather well-rounded minimum for the light-curve.

Maximum velocity, minimum velocity, and the velocity of the center of mass are +54, +4, and +32 km/sec., respectively.

There is evidence for greater amplitude of velocity variation in the lines whose chromospheric level in the sun averages 2700 km than in a contrasted group having a mean of about 550 km. On the other hand, $H\gamma$, chromospheric level 8000 km, has an amplitude no greater than that of the low-level lines.

The velocity-curve for $H\gamma$ is of special interest, for it seems to indicate a persistence of the maximum velocity of approach of its origin considerably beyond that of the other lines.

Spectrum and spectral changes.—The spectral class at median magnitude is about cG6, and has the small range cG4 to cG9 between maximum and minimum light.

The lines of hydrogen and those of the ionized atoms of certain elements attain their maximum intensity, relative to arc lines, at maximum light; but there is evidence that their minima precede minimum light, in some cases as much as ten days. The relation of relative intensity to phase for four pairs of lines is shown in Figure 2. Curves of photographic density for the spectral region λ 4325 to λ 4352 made with the Hartmann microphotometer from five plates for differing phases are given in Figure 3.

A variation in effective wave-length derived from the continuous spectrum at different phases agrees qualitatively with the evidence afforded by light-curves for different wave-length in that both show the star to be decidedly bluest at maximum light.

THE LIGHT-CURVE

This star, B.D.+7°1273, numbered 44990 in the new *Henry Draper Catalogue*, has the co-ordinates for 1900, $\alpha = 6^h19^m8$, $\delta = +7° 8'$.

[1] *Contributions from the Mount Wilson Observatory, Carnegie Institution of Washington*, No. 340.

In 1872 Gould[1] announced that it was variable after he and his assistants at the Cordoba Observatory had noted that it was then about a magnitude fainter than it had been the year previous. A few years later Davis, one of these assistants, obtained the period $27^{d}.0054$ and an interval between minimum and maximum light $(M-m)$ equal to 8.5 days. His observations showed that the light variations are akin to those of δ Cephei. The star was assigned the designation T Monocerotis and is of rather more than ordinary interest, because its period is one of the longest of the Cepheid variables.

Subsequent work by various other observers confirmed the Cepheid characteristics and agreed in general with Davis' results, although differences in detail exist. Among these may be mentioned differences in the values of $M-m$, an inflection in the light-curve about ten days after maximum light, different values for maxima and minima at different epochs, and increasing values for the period as later measures became available for comparison with the first observations.

Probably the most reliable light-curves are those from observations by E. C. Pickering[2] and O. C. Wendell,[3] respectively. The former made eighty-six observations with a meridian photometer in nine out of sixteen consecutive cycles (1896–1898), and the latter two hundred observations with polarizing photometers in each one of five consecutive cycles (1899–1900). Both light-curves, especially that of Wendell, are nearly regular in shape, and together include almost continuous observation over an interval of more than three years. They are strong evidence against an inflection at ten days after maximum light, give good agreement for repeated maxima and minima, and establish with considerable certainty the value for $M-m$. In consequence, the mean light-curve defined by Wendell's observations has been adopted here and appears in Figure 1. His maximum is 5.61 mag., minimum 6.77 mag., and the interval $M-m$ is seven days.

The question of the lengthening of the period has been studied by Bemporad,[4] who has collected representative maxima that have

[1] *American Journal of Science* (3), **4**, 477, 1872.

[2] *Harvard Annals*, **46**, 122, 135, 145, 151, 155, 158, 160. [3] *Ibid.*, **69**, 42.

[4] *Memorie della Società Astronomica Italiana* (Nuova Serie), **1**, 229, 1920.

been satisfactorily determined in the interval 1874–1920 inclusive. To these may now be added a maximum determined by Gallisot,[1]

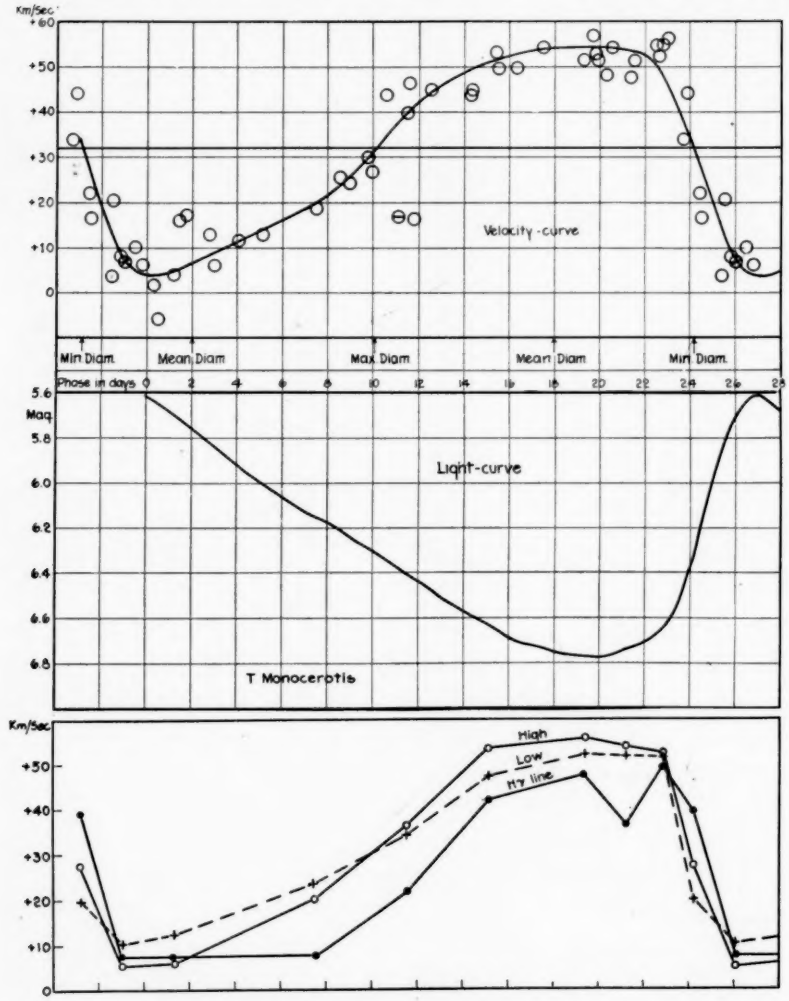

FIG. 1.—T Monocerotis. Top, velocity-curve. Middle, Wendell's light-curve. Bottom, velocity-curves from high- and low-level lines and from $H\gamma$.

and another from the radial velocities, by assuming coincidence of maximum light and minimum velocity.

[1] *Bulletin astronomique, mémoires et variétés*, **3**, 207, 1923.

The first and second columns of Table I list the photometric observer and the maximum which he determined. The third, fourth, and fifth columns show the differences between observed maxima and maxima computed from the three formulae given at the foot of the table. The period used in formula I was found from the Mount Wilson radial velocities alone; formula II is that derived by Bemporad in the paper already cited; and formula III is identical with II except for a change in the coefficient of E^2. The first, typical of a

TABLE I

T MONOCEROTIS—REPRESENTATION OF MAXIMA

Observer	J.D. of Maximum	O−C		
		I	II	III
Davis	2405556.62	$+2^d.26$	$-0^d.61$	$-0^d.74$
Sawyer	9040.13	0.56	+ .02	+ .02
Sawyer	2410012.19	0.00	.00	.00
Sawyer / Yendell	2442.53	−1.20	− .12	− .26
Pickering	4144.25	1.56	+ .09	.01
Wendell	5089.60	1.81	.08	.07
Nijland	7628.83	2.20	+ .09	.26
Bemporad I	8412.10	2.42	− .09	.51
Bemporad II	2422357.00	2.03	+0.03	− .89
Gallisot	2737.03	0.25	1.72	+ .76
Sanford	3790.35	−0.58	+1.14	0.00

Formula I (Sanford) ..... Max=J.D. 2410012.19+27.017149E, G.M.T.

Formula II (Bemporad) ..... Max=J.D. 2410012.1956+ 27.003131E+0.00002084$1E^2$, G.M.T.

Formula III (Bemporad modified) .... Max=J.D. 2410012.1956+ 27.003131E+0.00002522$1E^2$, G.M.T.

formula with a constant period, evidently leaves something to be desired; II does very well except for the two maxima that I have added; and III gives no residual greater than $0^d.9$. The last has been adopted. Whether this will continue to predict maxima in the future, or is merely an approximation to a portion of a periodic change in the period, can only be decided after the lapse of a considerable interval.

THE RADIAL-VELOCITY CURVES

Forty-seven slit spectrograms of T Monocerotis have been obtained with the 60-inch and 100-inch reflectors during the interval 1917–1927. Table II gives the data of these observations. The plate

TABLE II

OBSERVATIONS OF T MONOCEROTIS

Plate	Date	G.M.T.	Phase	Vel.	Remarks
				km/sec.	
γ 6373..	1917 Nov. 23	21^h57^m	$9^d.784$	+29.8	Very good
6384..	25	22 25	11.803	16.4	Very good
6434..	Dec. 3	23 40	10.855	53.0	Poor
6513..	30	20 49	19.712	56.8	Fair
6690..	1918 Feb. 1	17 49	25.562	20.7	Good
12334..	1923 Dec. 16	20 18	7.521	18.7	Good
12340..	17	20 30	8.530	25.6	Good
12350..	20	20 26	11.528	39.8	Poor
C 2592..	24	20 47	15.538	49.7	Good
γ 12406..	1924 Jan. 17	21 43	12.553	45.0	Fair
12416..	19	16 10	14.321	43.9	Poor
C 2642..	20	18 51	15.433	53.1	Fair
γ 12448..	26	17 28	21.376	47.6	Good (over-exposed)
12531..	Mar. 18	17 35	19.323	51.4	Poor
12538..	19	16 47	20.290	48.2	Poor
13029..	Oct. 16	0 42	14.385	44.9	Fair
13257..	1925 Feb. 9	18 54	23.026	56.3	Good
C 3197..	Mar. 11	15 10	25.842	8.2	Good (over-exposed)
C 3201..	12	15 01	26.836	6.3	Good (over-exposed)
γ 13365..	Apr. 11	15 38	2.811	12.8	Good
13822..	Oct. 7	23 30	19.950	51.4	Fair
13829..	9	0 33	20.994	53.4	Good (over-exposed)
C 3592..	Dec. 3	21 29	22.806	54.9	Poor
γ 13958..	1926 Jan. 2	20 05	25.717	16.4	Good density: poor focus
13980..	5	21 50	1.759	17.3	Good
14003..	26	18 34	22.623	52.3	Good (fogged)
14013..	27	20 21	22.697	34.0	Very good
14051..	Feb. 24	17 37	24.537	16.8	Good
14056..	25	15 17	25.430	3.8	Good
C 3713..	26	16 48	26.498	+10.3	Good
γ 14066..	27	16 57	0.496	− 5.7	Good
γ 14073..	28	15 53	1.449	+16.3	Fair
γ 14090..	Mar. 22	15 32	23.437	44.2	Good
γ 14098..	23	15 27	24.434	22.1	Good (over-exposed)
C 3999..	Sept. 15	0 16	10.587	43.8	Poor
C 4005..	16	0 25	11.594	46.4	Poor
C 4063..	Oct. 22	0 17	20.558	54.2	Good
γ 14627..	22	22 23	21.541	51.3	Good
14634..	24	0 27	22.565	54.7	Good
14684..	Nov. 13	20 15	16.359	49.7	Poor
14697..	14	23 52	17.510	54.2	Fair
14787..	1927 Jan. 17	21 25	0.314	1.9	7-inch camera;* very strong
14792..	18	18 54	1.210	4.0	7-inch camera;* very strong
14822..	Feb. 17	15 46	4.048	11.6	Good
14854..	Mar. 15	15 33	3.008	6.2	Very good
C 4230..	Apr. 17	15 41	8.983	24.3	Good
4237..	18	15 37	9.981	+26.7	Good stellar, poor comparison spectrum

* Dispersion about one-half that of the other plates.

numbers are in the first column, wherein the prefix C identifies spectrograms made with the 100-inch reflector and γ those taken with the 60-inch reflector. All but two noted in the table have an approximate dispersion of 36 A per millimeter at $H\gamma$.

Forty-seven lines between λ 4215 and λ 4571, together with the lines $H\delta$ and $H\beta$, have been used for deriving the radial velocities. These lines were chosen from those available within the spectral region in question so as to be as free as possible from troublesome blends, and yet be sufficiently numerous to furnish data regarding velocities derived separately from high-level, low-level, enhanced, and hydrogen lines. More will be said on this point later. The wave-lengths for the lines selected have been determined from measures upon eight plates whose velocities, as derived from tables used in our general radial-velocity work, are approximately midway between the maximum and minimum velocity for this variable. The fifth column in Table II gives the velocities measured with the use of these wave-lengths, exclusive of the hydrogen lines.

In addition to velocities in Table II, Frost[1] has published the three following values:

Date	G.M.T.	Phase	Vel.
			km/sec.
1905 Nov. 3.....	21^h30^m	11.116	+17
24.....	21 40	5.107	13
Dec. 15.....	20 30	26.056	+ 7

We have, therefore, fifty values of the radial velocity extending from 1905 to 1927, from which to derive a radial-velocity curve. Efforts to combine the velocities into a single cycle by means of a period of constant length produce neither a smooth run of Mount Wilson observations nor a satisfactory utilization of the Yerkes velocities. Since the modified formula of Bemporad represents the observed light maxima so well, it was tried for grouping the radial velocities and found to improve the smoothness of the Mount Wilson observations and to harmonize the Yerkes values with these. This method of assembling the observations was therefore adopted, and

[1] *Astrophysical Journal*, **23**, 266, 1906.

the phases given for both Mount Wilson and Yerkes plates are so derived. The top of Figure 1 shows the individual observations plotted as circles (Mount Wilson) and barred circles (Yerkes). The freehand curve through them is deemed a fair approximation to the actual velocity-curve. Of the two very discrepant values of the radial velocity shown at slightly more than eleven days after minimum velocity, one is the first value given by Frost, which he remarked is the least accurate of his three; the other is derived from one of the best Mount Wilson plates, γ 6384, and its discordance remains unexplained.

The coincidence of minimum velocity with zero phase is of course to be expected, since the modification of Bemporad's formula was largely to satisfy the epoch of observed minimum velocity (assumed to represent maximum light). The fact that such a formula brings all the radial velocities together into a satisfactory velocity-curve, although the first and last observations are separated by almost twenty-two years, seems to justify the assumption.

The radial-velocity curve may be compared with Wendell's light-curve, which is shown below the velocity-curve in Figure 1. The accordance of maximum light and minimum velocity has already been mentioned. The agreement of minimum light and maximum velocity is no less precise. Two differences, however, are to be noted: one, the contrast of a smooth progression in light-variation with what appears to be a well-marked inflection in the radial-velocity curve at about phase ten days; and the other, the well-rounded minimum of light as compared with the blunt maximum of the velocity-curve, followed as it is by a very rapid fall to minimum velocity. The inflection in the velocity-curve resembles that found in the curves for such Cepheids as W Sagitarii,[1] ζ Geminorum,[2] and η Aquilae,[3] and hence is not at all an abnormal feature. It also brings to mind the inflection found by some observers in the light-curve of T Monocerotis, although little dependence is to be placed on this because the most accurate observations do not show the inflection.

Around the times of both maximum and minimum velocity, especially the latter, the individual values of radial velocity show a

[1] *Lick Observatory Bulletins*, **3**, 35, 1904.

[2] *Ibid.*, **12**, 148, 1926.

[3] *Ibid.*, p. 147, 1926.

considerable spread. To seek an explanation of this in the assumption that the velocity-curve is not always precisely the same seems hardly justified, for some of the differences in residuals for plates close together in the same cycle are about as large as any to be found between spectrograms made in different cycles. Large dispersion in radial velocity at maximum light is not, however, peculiar to this Cepheid, as may be verified by a glance at the radial-velocity curves for X Sagittarii,[1] Y Sagittarii,[2] and W Sagittarii,[3] for example.

The usual elements of elliptic motion have not been determined because (as evident at a glance) they could give only a crude approximation to the observations, and because such an interpretation of the curve is open to serious question. Maximum velocity, minimum velocity, and the center-of-mass velocity are +54, +4, and +32 km/sec., respectively, the last being that velocity which divides the velocity-curve into equal areas.

It is interesting to note the phases, indicated below the velocity diagram, for which, on the pulsation hypothesis, the star has its mean, maximum, and minimum diameters. Minimum diameter corresponds approximately to the phase of most rapid change in radial velocity on the downward slope, and maximum diameter is closely associated with the phase of most rapid change on the upward branch.

Furthermore, it may be noted incidentally that the curve can be resolved into two typical radial-velocity curves, each having a period equal to the photometric period. One curve would have a semi-amplitude of 20 km/sec. and a so-called periastron point at about twenty-four days after maximum light, and the other, a semi-amplitude of 8.5 km/sec. and periastron at about ten days after maximum light. It is merely pointed out that the curve may be so resolved, without inquiring whether such a procedure is legitimate, or, if legitimate, what the explanation may be.

From the foregoing paragraphs it may therefore be stated that the relation of the general velocity-curve to the mean light-curve for T Monocerotis is quite normal when compared with the results for numerous other Cepheid variables, for the most part of shorter period.

Various members of the staff of the Observatory of the Univer-

[1] *Ibid.*, **5**, 113, 1909. [2] *Ibid.*, p. 84, 1908. [3] *Ibid.*, **3**, 35, 1904.

sity of Michigan have derived velocity-curves for certain Cepheids from different groups of lines, on the assumption that such treatment might possibly throw some light upon the pulsation theory of Cepheid variation. Adequate approach to this problem demands the highest practicable dispersion and resolving power, applied to the very brightest Cepheids. Nevertheless, it is probable that for some time, at least, the Mount Wilson observations here considered will be the only source from which to derive even qualitative results for T Monocerotis, whose rather long period makes it of considerable interest in this as in other respects. Such is the only justification for presenting the following discussion, which has been limited to deriving velocity-curves from (1) lines of high atmospheric level, (2) lines of low atmospheric level, and (3) the γ line of hydrogen.

The lines have been chosen from the list of forty-seven lines according to heights assigned on the basis of Mitchell's[1] levels in the sun. The approximate mean level thus found for the first group (twenty-one lines) is about 2700 km; for the second group (nine lines), 550 km; and for $H\gamma$, 8000 km. $H\gamma$ alone was used since it is the only hydrogen line consistently measured at all phases. In order to minimize somewhat the accidental differences, the measures are grouped into nine normal places.

The velocity-curves defined by the normal places for each of the three classes of lines are shown at the bottom of Figure 1. Both high- and low-level curves resemble the general curve at the top of Figure 1, even after the drastic smoothing effected by the use of so small a number of normal places. The one point of interest seems to be a consistently smaller amplitude for the velocities from low-level lines as compared with those from high levels.

The velocity-curve derived from $H\gamma$ (and this is not essentially different when the data for $H\delta$ and $H\beta$ are considered), although it is representative of a still higher level, shows an amplitude at least not greater than that given by low-level lines. The three curves do not, therefore, show a steady progression in amplitude with increase in level.

By itself, the $H\gamma$ curve is of interest as pointing toward a lag after maximum velocity, as though the portion of the stellar atmosphere

[1] *Astrophysical Journal*, **38**, 407, 1913.

responsible for the $H\gamma$ line continued its most rapid approach to a much later phase than those portions associated with the other lines. About minimum light the deviations from the general curve are probably small. Although the two normal places just preceding the drop to minimum velocity both include several values which are fairly consistent, the reality of the depression which they show in the $H\gamma$ velocity-curve at phase twenty-one days is probably open to serious question.

A proper discussion of the radial-velocity variation shown by the enhanced lines undoubtedly requires a more elaborate classification than the number of lines here measured will warrant. All that can be said is that a group of titanium enhanced lines seems to give a velocity-curve differing little from the general curve, except perhaps in amplitude, which appears to be intermediate between that of the high- and the low-level curves, and probably somewhat nearer the value for the latter.

SPECTRUM AND SPECTRAL CHANGES

The spectral class of T Monocerotis is cG6 at median magnitude, with a variation from cG4 to cG9, according to the classification of Adams and his collaborators at Mount Wilson. As in other Cepheids, the enhanced lines of such elements as titanium, iron, strontium, scandium, etc., and the Balmer lines of hydrogen are conspicuous at all phases, but especially near maximum, when they attain maximum intensity.

In an attempt to fix the light-phases for maximum and minimum intensity of the absorption lines, measures have been made with the Hartmann microphotometer as arranged by Pettit for use with thermocouple and galvanometer. These measures have been made both visually and photographically by comparing galvanometer deflections for the sensitive lines with the deflections for certain arc lines. When these comparisons are plotted, the phase for maximum intensity seems to be fixed with considerable certainty at maximum light. On the other hand, the phases for which the sensitive enhanced and hydrogen lines are weakest, as compared with their arc standards, do not appear either to agree with one another or to approximate at all closely the phase of minimum light. In general, it may

be said that minimum intensity is attained not later than minimum light, and in several cases seems to anticipate that phase, sometimes by as much as ten days.

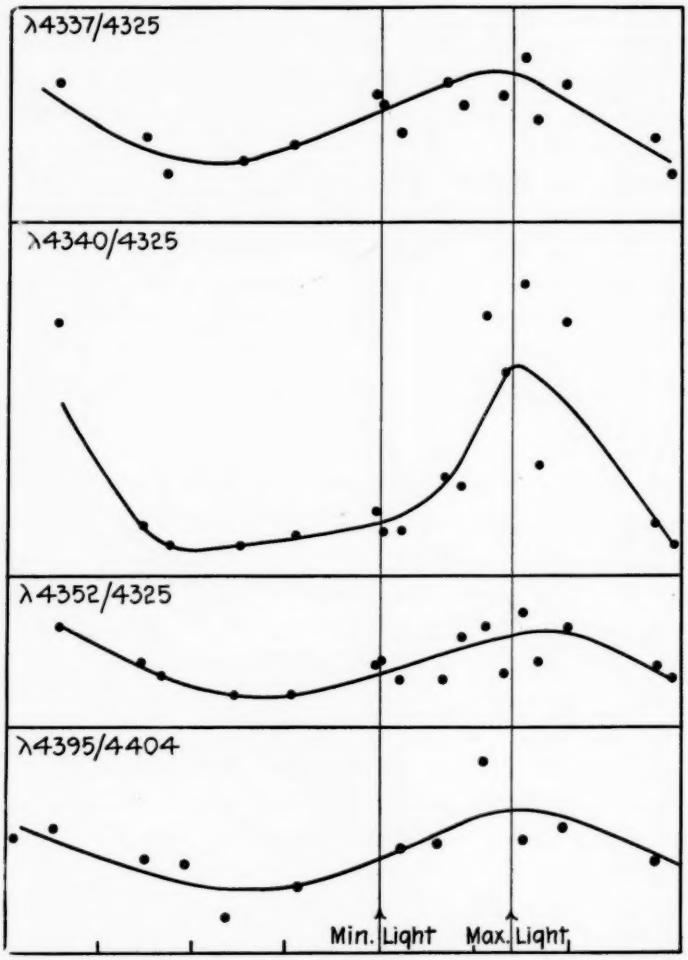

FIG. 2.—Changes of relative intensity with phase for four pairs of lines in the spectrum of T Monocerotis.

These relations of relative intensity to phase are shown qualitatively by the four curves in Figure 2, derived with the aid of the Hartmann microphotometer. The first three curves compare the strength of λ 4337 (Ti^+), λ 4340 ($H\gamma$), and λ 4352 (Ti^+), respective-

ly, with that of λ 4325. In the last case λ 4395 (Ti^+) has been compared with λ 4404. Both λ 4325 and λ 4404 are strong lines from the neutral atom of iron. In the first three cases, the areas of the respective intensity-curves in terms of the area for λ 4325, photographically registered, have been plotted against phase. For the fourth case the visually observed galvanometer deflections of λ 4395, in terms of those of λ 4404, have likewise been plotted against phase. The points refer to single measures upon individual plates scattered over all phases and chosen for the general density best suited to the purpose. The maximum intensity in all four cases falls close to the phase of maximum light, but minimum intensity, for these four cases at least, seems to precede minimum light very considerably—by ten or eleven days in the case of $H\gamma$. $H\gamma$ then remains practically at minimum intensity until minimum light. Apparently, therefore, $H\gamma$ is more or less stable at minimum intensity for one-half the light-cycle, and then undergoes a rapid increase to maximum intensity at maximum light and a decrease to minimum, all in the other half of the light-cycle. For the three enhanced titanium lines a much steadier progression takes place, so that a fairly definite minimum is marked out seven or eight days before minimum light, after which the increase in relative intensity begins again. Other lines which were measured show the same trend, but these four have the most pronounced and most easily measurable changes with phase, and are reproduced for this reason. It should be kept in mind that these curves denote changes in relative intensity and are not necessarily to be interpreted as measures of the real changes, for they may be complicated by changes in the comparison lines.

Five different intensity-curves covering the spectral region λ 4325 to λ 4352 are illustrated in Figure 3, the last of the six curves being the same as the first. These have been traced from photographic intensity-curves made with the registering Hartmann microphotometer. A depression indicates an absorption line or a blend, and all such features fit for micrometric measurement, and several besides are consistently recorded. A number of lines of interest have been marked, and it is easy to trace several striking changes of relative intensity with phase. The most impressive change is, of course, in the $H\gamma$ line. These five curves, with those similarly ob-

tained from fourteen other spectrograms, are the basis of the first three curves in Figure 2.

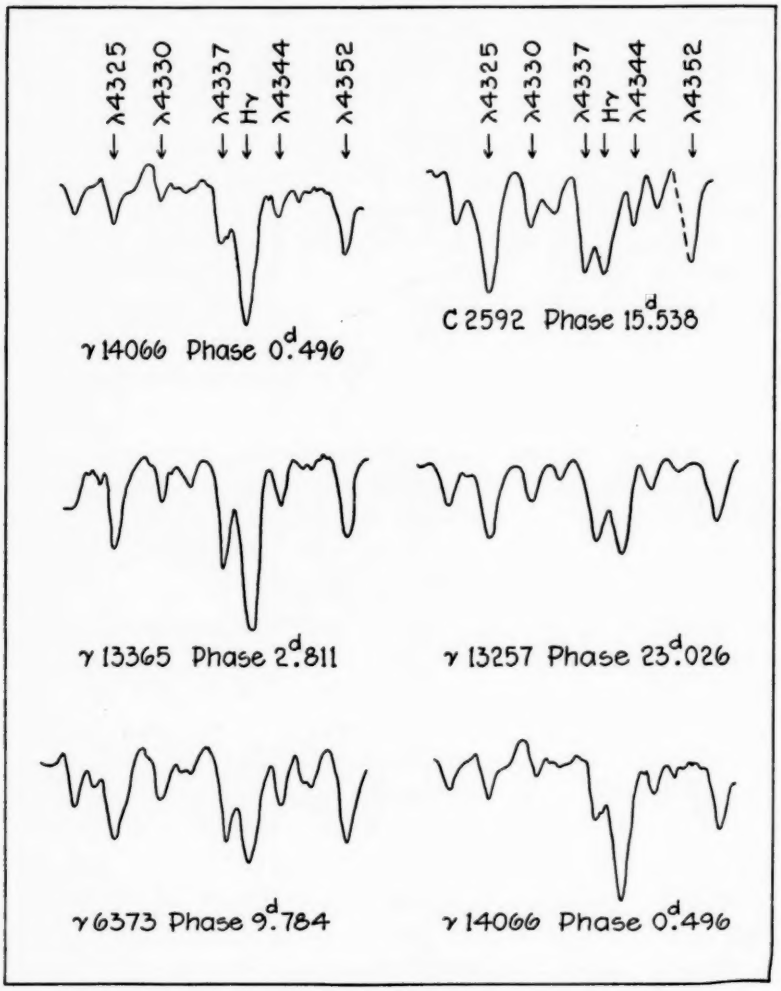

FIG. 3.—Microphotograms of the spectral region λ4325 to λ4352, inclusive, for different phases of the velocity variation in T Monocerotis.

In addition to the small change in spectral type and the change in the relative intensity of enhanced lines to arc lines (the two variations already treated), there is a definite change in effective wave-

length with phase, so that the star is decidedly bluest at maximum light. Gallisot[1] measured this change with a Nordmann photometer, using three types of screens effective in giving measures of the star's brightness in each of three more or less isolated spectral regions, which are (*R*) from λ 5900 to the infra-red; (*V*) from λ 4900 to λ 5900; and (*B*) from λ 4900 to the ultra-violet. The light-curves thus derived gave amplitudes of 0.73, 1.00, and 1.28 mag., respectively, and hence show a marked difference in color at different phases—a well-established result for many Cepheids.

I have endeavored to estimate the wave-length at the violet end to which each spectrogram would be capable of wave-length measurement if the density at about λ 4600 had been ideal. Although it is recognized that many factors besides the effective wave-length of the star may modify this, the mean curve giving the relation of this wave-length to phase may still be of some value. It indicates that from about eight days after maximum to the phase of minimum light the star changes little in color, and that the extension to the violet limit on the basis outlined above is approximately 4250 A. From minimum, or very shortly after, the effective wave-length moves toward the violet, becomes somewhat less than $H\delta$ about maximum light, and then turns back to the value 4250 A at some eight days after maximum light. This result, crudely derived from the spectrograms, together with the shape of the light-curves which Gallisot obtained for different screens, leads to the remark that the star is "decidedly bluest at maximum light," rather than to the statement that it is "reddest at minimum light." The change in effective wave-length appears to bear some analogy to the anomalies found in both the velocity-curve and the relative intensity for $H\gamma$ shown in Figures 1 and 2, respectively.

CARNEGIE INSTITUTION OF WASHINGTON
MOUNT WILSON OBSERVATORY
July 1927

[1] *Bulletin astronomique, mémoires et variétés*, **3**, 207, 1923.

RELATED LINES IN THE SPECTRA OF THE ELEMENTS OF THE IRON GROUP[1]

By HENRY NORRIS RUSSELL[2]

ABSTRACT

Homologous lines.—Recent theories of spectral structure suffice to identify those groups of homologous lines in the spectra of different elements which arise *from similar electronic transitions* within the atoms. Such groups have quite different spectroscopic names and multiplicities, but they show very *similar* physical and astrophysical *behavior*.

Tables are given of the *homologous terms* in the *arc spectra* from *K* to *Zn* and in the *spark spectra* from Ca^+ to Zn^+. The identifications of the lower terms follow Hund; those of many of the higher terms are new. The relations of the terms are illustrated graphically, thus clearing up certain doubtful questions.

Tables are also given of the *homologous lines* which arise from eight different electronic transitions in the neutral, and four in the ionized atom.

The transition from a 4p to a 4s orbit accounts for most of the strongest lines in both the arc and spark spectra. These lines shift steadily toward the ultra violet as the atomic number increases.

Transitions from a 5s to a 4p orbit give arc lines in the visible region, some of which are strong, while others make it possible to determine the ionization potential. Many other sets of homologous lines may be identified when the spectra have been more completely analyzed.

Relations between different spectra.—If the elements of the iron group are written as follows

K	*Ca*	*Sc*	*Ti*	*V*	*Cr*	*Mn*
Zn	*Cu*	*Ni*	*Co*	*Fe*	*Mn*	*Cr*

the spectrum of any element contains a large portion which is very similar to a corresponding portion of the element above or below, and one step to the right, and another portion similarly related to a part of that of the element above or below and to the left. Each spectrum also contains other portions peculiar to itself.

1. INTRODUCTION

It has long been recognized that the spectra of elements belonging in the same column of the periodic table are so similar that they can be correlated almost line by line. For example, the homology of *Ca* 4226, *Sr* 4607, *Ba* 5535, or of Ca^+ 3933, 3968, Sr^+ 4077, 4215, Ba^+ 4554, 4934, is a commonplace. The spectra of elements in the same row of the periodic table, however, present no apparent points of resemblance, nor did even their successful analysis, after the laws of multiplet structure were discovered, bring out much obvious similarity. The lowest spectroscopic term, corresponding to the nor-

[1] *Contributions from the Mount Wilson Observatory, Carnegie Institution of Washington*, No. 341.

[2] Research Associate of the Mount Wilson Observatory, Carnegie Institution of Washington.

mal state of the atom, may be of the types S, P, D, or F and belong to a system of any multiplicity from singlets to septets.

Order was recognized in the apparent chaos only when the work of several investigators, culminating in that of Hund,[1] traced the relation of these spectroscopic terms to the electronic configurations in the atom which produced them. It then became evident that our previous difficulties had arisen because we were seeking for similar spectroscopic terms, whereas we should have sought for lines produced by similar transitions within the atom. When once this is understood, very striking relations appear between spectra and between individual groups of lines which have previously seemed to be quite unconnected.

These new relations are especially well illustrated in the spectra of the elements in the earlier part of the first long period—from *K* to *Zn*—which are often called the "iron group."

2. SKETCH OF THE THEORY

In this group the complete inner shells include electron orbits[2] of types 1s, 2s, 2p, 3s, 3p, and the outer incomplete shell is formed, in the normal states of the neutral and ionized atoms, of electrons with 4s or 3d orbits—two of the former being first added in *K* and *Ca*, followed by ten of the latter from *Sc* to *Zn*. In the low metastable energy states, which are numerous in most of these atoms, only 4s and 3d electrons are present outside the completed shells. The corresponding terms are all "even" and do not combine with one another to give spectral lines; but they combine freely with higher "odd" terms arising from configurations including a 4p electron; and these again combine with still higher even terms coming from configurations in which one electron is in a 5s or 4d orbit. Few configurations involving higher orbits (6s, 5p, 5d, 4f, etc.) are known, except in the spectra in which series are prominent. Those including an odd number of p and f electrons (taken together) are "odd."

Configurations of this sort may be represented by symbols such as $(4s)^2(3d)^5(4p)$, in which the exponents denote the number of electrons of the given type which are present. We may abbreviate

[1] For a full account see F. Hund, *Linienspektren und periodisches System der Elemente* (Berlin, 1927).

[2] This familiar nomenclature is used for convenience, without thought of opposition to the newer wave-mechanics.

this for our present purpose into $s^2\,d^5\,p$, and denote configurations involving a more highly excited electron (where we shall have to consider only 5s and 4d) by expressions such as $s^2d^5 \cdot s$, in full, $(4s)^2$-$(3d)^5(5s)$. Not more than two s electrons of the same total quantum number (e.g., 4s) can be present in any atom, but the number of similar d electrons may run up to ten. Six 4p electrons might be present—and actually are in *Kr;* but we shall not have to deal with more than two of them in the iron group. In a transition accompanied by the production of a spectral line, one electron must "jump" by one step—from s to p or p to d—and one other may sometimes simultaneously jump by two steps—from s to d, in this case. We may therefore arrange the configurations with which we have to deal in three groups as follows:

I	II	III	
$d^{n-2}\,s^2$	$d^{n-2}\,s\,p$	$d^{n-2}\,s \cdot s$	$d^{n-1} \cdot s$
$d^{n-1}\,s$	$d^{n-1}\,p$	$d^{n-2}\,s \cdot d$	$d^{n-1} \cdot d$
d^n	$d^{n-1}\,f$	$d^{n-2}\,p^2$	

These represent the important configurations for an atom which, in its neutral state, has n outer electrons and the atomic number $n+18$. In the present paper "n" will be used in this sense throughout, so that the configurations I in the singly ionized atom will be denoted by $d^{n-3}\,s^2$, $d^{n-2}\,s$, d^{n-1}.

In general, the first group of configurations will give the even terms of lowest energy (since the 4s and 3d electrons are most firmly bound); those of the second will give "odd" terms at a middle level; and the third, high-lying "even" terms.

Spectral lines arise only from transitions between odd and even terms; for example, $d^{n-1}\,s - d^{n-1}\,p$ or $d^{n-2}\,s^2 - d^{n-1}\,p$. The first of these transitions, which demands only the jumping of one electron from a p to an s orbit, is likely to give much stronger lines than the second, which involves the simultaneous jumping of two electrons, one from d to s and the other from p to s.

If now we vary n—that is, the atomic number—we shall have a series of transitions between states in successive elements of the periodic table in each of which the electron jump is essentially the same; and it is such transitions which produce the really homologous lines in the successive spectra.

These homologous configurations give rise, however, to apparently quite dissimilar spectroscopic terms. In accordance with Pauli's restriction, groups of 3d electrons produce the following terms:[1]

d^{10}	^1S	
d,d^9	^2D	
d^2,d^8	$^3F',^3P'$;	$^1G,^1D,^1S$
d^3,d^7	$^4F',^4P'$;	$^2H',^2G,^2F',^2D,^2P',^2D$
d^4,d^6	^5D ;	$^3H',^3G,^3F',^3D,^3P',^3F',^3P'$, etc.
d^5	^6S ;	$^4G,^4F',^4D,^4P'$ ....., etc.

Many terms of lower multiplicity, which do not now concern us, are omitted. The terms given in the first column, which are of the highest multiplicity present, lie lowest, and the F′ term lower than the P′, when both are present. In the next group, the G term is usually, though not always, the lowest, and the H′, D, and P′ terms (so many as are present) are not much higher.

The addition of other electrons to these configurations converts each "parent term," such as those tabulated, into a group of terms, usually of different multiplicity and name (letter). In general, the multiplicity is both increased and diminished by a unit for each added electron. Adding an s electron leaves the letters unchanged. Adding a p electron converts each parent term into a triad of closely related terms. Thus a D term goes into PD′F terms (but an S term into a P term only). Adding a d electron produces, in general, groups of five terms (pentads). Thus F gives PD′FG′H (but P gives PD′F and S, D alone). The terms which originate from the same parent term are closely related, and the combinations between them account for most of the strong lines of the spectrum. When two or more similar electrons are added, Pauli's restriction operates upon them too. Thus the addition of two 4s electrons leaves both the multiplicity and the letter unchanged; that of two 4p's is equivalent to combinations with the terms $^3P'^1S^1D$—the first changes the multiplicity by $+2, 0, -2$, and the others by 0, while the letters follow the previous rules.

3. PRINCIPAL TERMS IN SPECTRA OF THE IRON GROUP

With this brief summary of the theory, we proceed to tabulate the principal terms in the spectra which we have to consider. A com-

[1] Hund, *op. cit.*, p. 119.

plete tabulation of the terms which are theoretically to be expected, and which have actually been found, in almost perfect agreement with theory, in those spectra which have been fully analyzed, would occupy far too much space. We may content ourselves, in general, with listing those terms which arise from the lowest energy levels of the singly and doubly ionized atoms. Experience shows that, at least for the elements here considered, the term of lowest energy level always comes from the configuration d^{n-2} and is the one which is first listed for the corresponding number of electrons in the preceding section. How the resulting terms in the arc and spark spectra arise from it may be illustrated in the typical case of titanium (n = 4).

The lowest energy state of *Ti* III is here a $^3F'$ term coming from the d^2 configuration. The results of adding s electrons are as follows:

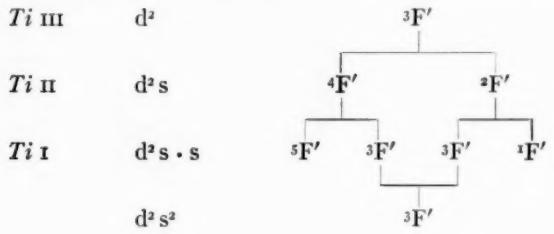

When the successive electrons which are added are unlike (4s and 5s), the original term splits up into four in *Ti* I; but when they are alike, Pauli's restriction abolishes the quintet and singlet terms and combines the triplet terms into one—which, however, is the leading member of both the series of $^3F'$ terms which may be obtained by adding 5s, 6s electrons (such series are actually known in several elements). On adding a p electron followed by a 4s electron or another p, we have

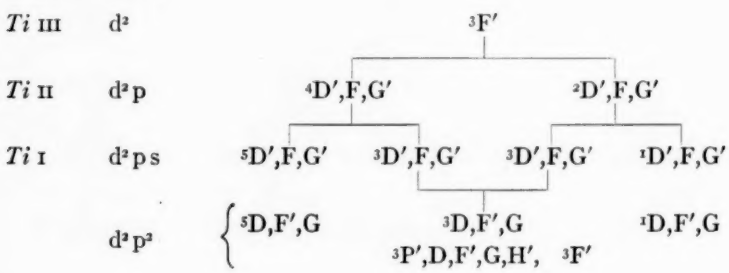

The addition of a 4d electron (unlike those already present) gives pentads:

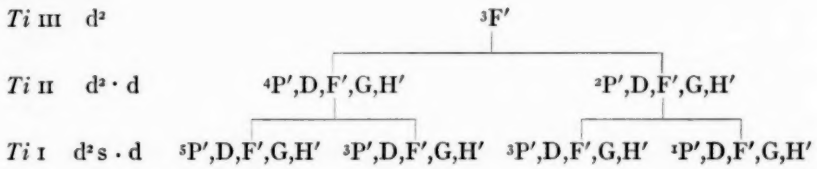

On adding a 3d electron Pauli's exclusion operates, and the list of terms from the d^3 configurations must be consulted. The resulting terms in *Ti* II have no such simple relation to the parent terms of *Ti* III as in the previous case; but they show families of their own. We give here only the derivatives of the lowest term:

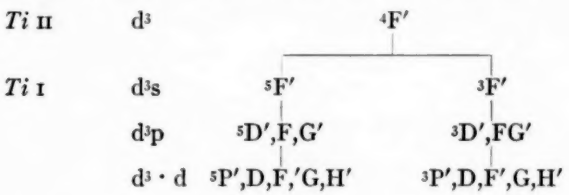

All the members of most of these groups, and some members, at least, of almost all of them, have actually been identified in *Ti* I and *Ti* II, along with many others arising from other parent terms of the d^2 and d^3 configurations. When an equally complete analysis has been made, the same will probably be true in all the other spectra.

Still another configuration, d^4 (in general d^n), may exist in the neutral *Ti* atom; but this gives high-lying terms of little importance, which thus far are known in but a few cases.

The principal low-level terms in the spectra of the first three stages of ionization are related as follows:

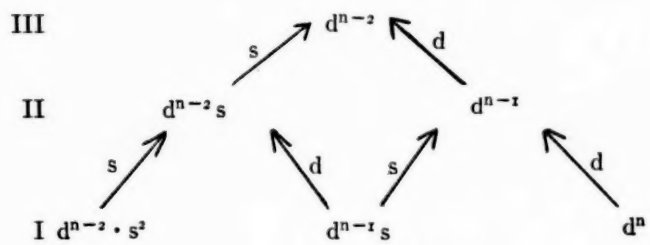

The arrows indicate the processes of ionization through which one state may be reached from another by removal of an electron. There are, therefore, two different ionization potentials for the spark spectra and four for the arc (three if the configuration d^n be neglected), and, of course, many more corresponding to transitions upward from other metastable terms, not here considered. In *K* and *Zn* the number of possible transitions is diminished by the limitation in the number of electrons as a complete group. The principal ionization potential is usually defined as the energy difference between the lowest (normal) states of the neutral and the ionized atom (and so on for higher ionizations). It should be especially remarked, however, that this quantity does not always correspond to the simple removal of one electron. Among the elements considered the normal state of the neutral atom belongs to $d^{n-2}\,s^2$, except for *K*, *Cr*, and *Cu;* in the ionized atom the state of lowest energy is $d^{n-2}\,s$ for *Ca*, *Sc*, *Ti*, *Mn*, and *Fe*, and d^{n-1} for the rest. In *V* and *Co*, therefore, the transition from one normal state to the other is from $d^{n-2}\,s^2$ to d^{n-1} and involves the removal of one electron and the shift of another.

4. TABLES OF THESE TERMS

The observed values of these principal terms in the arc and spark spectra of the elements from *K* to *Zn* are given in Tables I and II. The data have been collected from various sources,[1] and a few have been added by the writer, whose best thanks are due to his colleagues for generous permission to use valuable unpublished material. The values are counted upward from the lowest term of origin $d^{n-2}\,s^2$ in the arc (except for *K*, where there is no such term) or $d^{n-2}\,s$ in the spark. This unusual method has been adopted to make the regu-

[1] For papers up to 1926 see Hund, *op. cit.*, pp. 212–217; *Sc*, Sc^+, H. N. Russell and W. F. Meggers, *Scientific Papers of the Bureau of Standards*, **22**, 329 (No. 558), 1927; *Ti*, Ti^+, H. N. Russell, *Mt. Wilson Contr.*, Nos. 344, 345; *Astrophysical Journal*, **66**, 1927; *V*, V^+, W. F. Meggers, *Zeitschrift für Physik*, **39**, 114, 1926, and unpublished material; *Cr*, Cr^+, C. C. Kiess (unpublished); *Mn*, T. Dunham (unpublished); *Fe*, O. Laporte, *Proceedings of the National Academy of Sciences*, **12**, 496, 1926; Fe^+, H. N. Russell, *Mt. Wilson Contr.*, No. 318; *Astrophysical Journal*, **64**, 194, 1926; Co^+, W. F. Meggers (unpublished); Ni^+, A. G. Shenstone, *Physical Review*, **30**, 255, 1927; *Cu*, Cu^+, A. G. Shenstone, *Physical Review*, **28**, 449, 1926, and **29**, 380, 1927, and unpublished data.

TABLE I

Observed Terms and Origins, Arc Spectra

Configuration	n=1, *K*		n=2, *Ca*		n=3, *Sc*		n=4, *Ti*	
$d^{n-2}s^2$	.....	.....	^1S	0.0	^2D	168.3	$^3F'$	386.9
							$^3P'$	8602.4
$d^{n-2}sp$.....	.....	.....	^3P	15316.1	^4P	18571.4	$^5D'$	18695.2
					$^4D'$	16210.8	^5F	17215.4
					^4F	16026.5	$^5G'$	16458.7
					^2P	18855.8	$^3D'$	20126.1
					$^2D'$	16022.7	^3F	19574.0
					^2F	21085.8	$^3G'$	21739.7
			^1P	23652.4	^2P	24656.8	$^3D'$	25643.8
					$^2D'$	25014.2	^3F	25388.4
					^2F	25724.7	$^3G'$	30039.4
							$^1D'$	22081.2
							^1F	22404.7
							$^1G'$	24694.8
$d^{n-2}s\cdot s$	.....	.....	^3S	31539.7	^4D	34567.1	$^5F'$	36351.4
			^1S	33316.6	^2D	35745.6	$^3F'$	37824.7
					^2D	.....	$^3F'$	39785.9
							$^1F'$	41087.3
$d^{n-2}s\cdot d$	.....	.....	^3D	37757.8	^4S	.....	$^5P'$	42858.9
					$^4P'$	.....	^5D	42184.7
					^4D	39799.9	$^5F'$	43330.1
			^1D	37298.5	$^4F'$	40670.9	^5G	42019.2
					^4G	40028.2	$^5H'$	42205.6
$d^{n-2}p^2$	.....	.....	$^3P'$	38551.8	$^4P'$	.....	^5D	49036.5
			^1S	40690.6	^4D	.....	$^5F'$	48462.1
			^1D	40719.9	$^4F'$	45125.6	^5G	47446.8
$d^{n-2}sf$.....	.....	.....	^3F	42170.9	^4P	.....	$^5S'$	.....
			^1F	42343.5	to	.....	to	.....
					^4H	.....	$^5I'$	.....
$d^{n-1}s$	^2S	0.0	^3D	20371.3	$^4F'$	11677.3	$^5F'$	6843.0
					$^4P'$	.....	$^5P'$	14105.7
			^1D	21849.5	$^2F'$	15042.0	$^3F'$	11776.9
					$^2P'$	.....	$^3P'$	18911.6
$d^{n-1}p$	^2P	12985.1	^3P	39340.5	$^4D'$	32751.5	$^5D'$	30060.3
			$^3D'$	38259.5	^4F	31350.8	^5F	28896.1
			^3F	35897.2	$^4G'$	29303.5	$^5G'$	26910.7
			^1P	36731.5	$^2D'$	33707.3	$^3D'$	29912.3
			$^1D'$	35835.7	^2F	33278.6	^3F	27025.7
			^1F	40537.8	$^2G'$	33151.4	$^3G'$	27750.2
$d^{n-1}\cdot s$.....	^2S	21025.6	^3D	46704.0:	$^4F'$	42085.0	$^5F'$	39412.8
			^1D	.....	$^2F'$	.....	$^3F'$	.....
d^n.....	^2D	21535.6	$^3F'$	.....	$^4F'$	33906.4	^5D	.....
			$^3P'$	48563.7	$^4P'$	36572.7	.....	.....
$d^{n-1}\cdot d$.....	^2D	27397.6	^3S	51571.3	$^4P'$	.....	$^5P'$	.....
			$^3P'$	54304.6	^4D	.....	^5D	44381.2
			^3D	51396.3	$^4F'$	.....	$^5F'$	.....
			$^3F'$	.....	^4G	.....	^5G	45904.7
			^3G	.....	$^4H'$	.....	$^5H'$	44134.6

TABLE I—*Continued*

Configuration	n=5, *V*		n=6, *Cr*		n=7, *Mn*		n=8, *Fe*	
$d^{n-2}s^2$	$^4F'$	553.0	^5D	556.8	^6S	0.0	^5D	0.0
	$^4P'$	9824.6	.....	.....	.....	.....	.....	.....
$d^{n-2}sp$.....	$^6D'$	18438.1	^7P	20184.6	^8P	18705.4	^7P	23711.5
	^6F	18680.5	$^7D'$	20074.5	.....	.....	$^7D'$	19350.9
	$^6G'$	17136.4	^7F	18020.8	.....	.....	^7F	22650.4
	$^4D'$	21032.4	^5P	22074.0	^6P	24802.2	^5P	29056.3
	^4F	23519.8	$^5D'$	26065.3	.....	.....	$^5D'$	25900.0
	$^4G'$	22313.9	^5F	23529.3	.....	.....	^5F	26874.6
	$^4D'$	34747.0	^5P	33292.7	^6P	35769.9	^5P	36767.0
	^4F	33155.4	$^5D'$	34031.5	.....	.....	$^5D'$	39625.8
	$^4G'$	31937.0	^5F	33642.7	.....	.....	^5F	40257.3
	$^2D'$	.....	^3P	.....	^4P	31001.0	^3P	33947.0
	^2F	.....	$^3D'$	.....	.....	.....	$^3D'$	31322.6
	$^2G'$	.....	^3F	.....	.....	.....	^3F	31307.3
$d^{n-2}s{\cdot}s$.....	$^6F'$	37931.3	^7D	39208.4	^8S	39431.4	^7D	42815.8
	$^4F'$	39596.9	^5D	41073.6	^6S	41404.0	^5D	44677.0
	$^4F'$	.....	^5D	.....	^6S	49415.3	^5D	51350.5
	$^2F'$	.....	^3D	.....	^4S	49591.4	^3D	53747.5
$d^{n-2}s{\cdot}d$	$^6P'$	.....	^7S	.....	^8D	46712.6	^7S	.....
	^6D	.....	$^7P'$	.....	^6D	47207.3	$^7P'$	.....
	$^6F'$	.....	^7D	.....	.....	.....	^7D	.....
	^6G	.....	$^7F'$	.....	^6D	.....	$^7F'$	.....
	$^6H'$	.....	^7G	.....	^4D	.....	^7G	.....
$d^{n-2}p^2$	^6D	.....	$^7P'$	.....	$^8P'$	57086.2	$^7P'$	.....
	$^6F'$	.....	^7D	.....	.....	.....	^7D	.....
	^6G	.....	$^7F'$	.....	.....	.....	$^7F'$	.....
$d^{n-2}sf$.....	$^6S'$	.....	^7P	.....	^8F	52974.6	^7P	.....
	to		to				to	
	$^6I'$	.....	^7H	.....	.....	.....	^7H	.....
$d^{n-1}s$	^6D	2424.9	^7S	−7750.7	^6D	17052.3	$^5F'$	6928.3
							$^5P'$	17550.2
							$^3F'$	11976.3
	^4D	8715.7	^5S	− 157.6	^4D	23296.7	$^3P'$	22838.3
$d^{n-1}p$	^6P	24838.6	^7P	15748.2	^6P	44993.9	$^5D'$	33096.0
	$^6D'$	26738.3	.....	.....	$^6D'$	41789.5	^5F	33695.4
	^6F	25253.4	.....	.....	^6F	43313.3	$^5G'$	34844.0
	^4P	25130.9	^5P	19036.6	^4P	46901.1	$^3D'$	38175.4
	$^4D'$	26480.3	.....	.....	$^4D'$	45754.3	^3F	36686.2
	^4F	26172.0	.....	.....	^4F	44288.8	$^3G'$	35379.2
$d^{n-1}{\cdot}s$.....	^6D	.....	^7S	29145.1	^6D	56189.5	$^5F'$	47005.5
	^4D	.....	^5S	30132.4	^4D	57305.7	$^3F'$	47960.9
d^n.....	^6S	.....	^5D	.....	$^4F'$	.....	$^3F'$	.....
					$^4P'$	.....	$^3P'$	.....
$d^{n-1}{\cdot}d$.....	^6S	.....	^7D	34510.6	^6S	.....	$^5P'$	.....
	$^6P'$	.....	.....	.....	$^6P'$	.....	^5D	.....
	^6D	.....	.....	.....	^6D	.....	$^5F'$	.....
	$^6F'$	.....	^5D	.....	$^6F'$	.....	^5G	.....
	^6G	.....	.....	.....	^6G	.....	$^5H'$	.....

TABLE I—*Continued*

Configuration	n=9, *Co*		n=10, *Ni*		n=11, *Cu*		n=12, *Zn*	
$d^{n-2}s^2$	$^4F'$	0.0	$^3F'$	0.0	^2D	0.0	^1S	0.0
	$^4P'$	15184.0	$^3P'$	15609.8	.....	.....	.....	.....
$d^{n-2}sp$	$^6D'$	24627.8	$^5D'$	25753.6	^4P	27816.1	^3P	32890.5
	^6F	23611.7	^5F	28541.9	$^4D'$	32311.4	.....	.....
	$^6G'$	25138.8	$^5G'$	27261.0	^4F	29706.6	.....	.....
	$^4D'$	29294.5	$^3D'$	33500.8	^2P	34676.7	.....	.....
	^4F	28345.8	^3F	32973.3	$^2D'$	35395.8	.....	.....
	$^4G'$	28845.2	$^3G'$	30922.6	^2F	33760.7	.....	.....
	$^4D'$	39649.0	$^3D'$	.....	^2P	46746.7	^1P	46745.1
	^4F	41225.4	^3F	43258.7	$^2D'$	46916.8	.....	.....
	$^4G'$	41528.3	$^3G'$	43089.5	^2F	44827.2	.....	.....
	$^2D'$	33462.8	$^1D'$	36600.8	.....	.....	.....	.....
	^2F	31871.1	^1F	35639.1	.....	.....	.....	.....
	$^2G'$	31699.6	$^1G'$	33590.1	.....	.....	.....	.....
$d^{n-2}s{\cdot}s$	$^6F'$	45675.9	$^5F'$	48466.5	^4D	51200.7	^3S	53672.4
	$^4F'$	47524.4	$^3F'$	50466.1	^2D	53455.0	^1S	55788.1
	$^4F'$	.....	$^3F'$	.....	^2D	.....	.....	.....
	$^2F'$	.....	$^1F'$	50832.0:	.....	.....	.....	.....
$d^{n-2}s{\cdot}d$	$^6P'$	.....	$^5P'$	.....	^4S	59650.8	^3D	62778.1
	^6D	.....	^5D	.....	$^4P'$	59975.6	.....	.....
	$^6F'$	.....	$^5F'$	.....	^4D	60065.6	^1D	62458.2
	^6G	.....	^5G	.....	$^4F'$	60087.9	.....	.....
	$^6H'$	.....	$^5H'$	.....	^4G	59928.1	.....	.....
$d^{n-2}p^2$	^6D	.....	^5D	.....	$^4P'$	.....	$^3P'$	80395.3
	$^6F'$	.....	$^5F'$	.....	^4D	.....	.....	.....
	^6G	.....	^5G	.....	$^4F'$	.....	.....	.....
$d^{n-2}sf$	$^6S'$	.....	$^5S'$	.....	^4P	.....	^3F	68835.5
	to	.....	to	.....	to	.....	.....	.....
	$^6I'$	.....	$^5I'$	.....	^4H	.....	^1F	.....
$d^{n-1}s$	$^4F'$	3482.8	^3D	204.8	^2S	−11202.5	.....	.....
	$^4P'$	13795.4	.....	.....	.....	.....	.....	.....
	$^2F'$	7442.4	^1D	3410.0	.....	.....	.....	.....
	$^2P'$	16470.6:	.....	.....	.....	.....	.....	.....
$d^{n-1}p$	$^4D'$	32027.4	^3P	28569.3	^2P	19581.1	.....	.....
	^4F	32841.9	$^3D'$	29668.9	.....	.....	.....	.....
	$^4G'$	32430.6	^3F	29481.0	.....	.....	.....	.....
	$^2D'$	36092.4	^1P	32982.3	.....	.....	.....	.....
	^2F	35450.5	$^1D'$	31441.6	.....	.....	.....	.....
	$^2G'$	33439.6	^1F	31031.0	.....	.....	.....	.....
$d^{n-1}{\cdot}s$	$^4F'$	44782.0	^3D	42605.8	^2S	31934.4	.....	.....
	$^2F'$	45924.8	^1D	44262.5	.....	.....	.....	.....
d^n	^2D	.....	^1S	14728.9:	.....	.....	.....	.....
.....	.....	.....	.....	.....	.....	.....	.....	.....
$d^{n-1}{\cdot}d$	$^4P'$	.....	^3S	.....	.....	.....	.....	.....
	^4D	.....	$^3P'$	.....	.....	.....	.....	.....
	$^4F'$	.....	^3D	.....	^2D	38739.6	.....	.....
	^4G	.....	$^3F'$	.....	.....	.....	.....	.....
	$^4H'$	.....	^3G	.....	.....	.....	.....	.....

TABLE II

OBSERVED TERMS AND ORIGINS, SPARK SPECTRA

Configuration	n=2, Ca^+		n=3, Sc^+		n=4, Ti^+		n=5, V^+	
$d^{n-2}s$	^2S	0.0	^3D	177.6	$^4F'$	393.2	$^5F'$	557.9
					$^4P'$	10024.7	$^5P'$	11136.5
			^1D	2541.0	$^2F'$	4897.6	$^3F'$	6492.6
					$^2P'$	16625.3	$^3P'$	.....
d^{n-1}.....	^2D	13711.0	$^3F'$	4987.6	$^4F'$	1215.6	^5D	−2265.4
			$^3P'$	12154.3	$^4P'$	9518.0	.....	.....
$d^{n-3}s^2$	.....	.....	^1S	.....	^2D	25193.0	$^3F'$	.....
$d^{n-2}p$	^2P	25414.4	^3P	29823.9	$^4D'$	32767.0	$^5D'$	34925.9
			$^3D'$	28161.0	^4F	31300.9	^5F	34747.7
			^3F	27841.2	$^4G'$	30240.7	$^5G'$	32878.7
			^1P	30815.7	$^2D'$	32025.5	$^3D'$	34314.1
			$^1D'$	26081.3	^2F	31490.8	^3F	37824.8
			^1F	32350.0	$^2G'$	34748.5	$^3G'$	37007.7
$d^{n-3}sp$.....	.....	.....	^3P	39344.9	^4P	56325.9	$^5D'$	.....
					$^4D'$	52631.1	^5F	.....
					^4F	.....	$^5G'$	.....
			^1P	.....	^2P	.....	$^3D'$	.....
					$^2D'$	69622.1	^3F	.....
					^2F	70893.0	$^3G'$	.....
$d^{n-2}s$.....	^2S	52167.0	^3D	57743.4	$^4F'$	62594.3	$^5F'$	.....
			^1D	58251.9	$^2F'$	63444.8	$^3F'$	.....
$d^{n-2}d$.....	^2D	56858.4	^3S	61071.1	$^4P'$	.....	$^5P'$	.....
			$^3P'$	64705.2	^4D	66996.7	^5D	.....
			^3D	60001.6	$^4F'$	69081.4	$^5F'$	.....
			$^3F'$	63527.7	^4G	65241.6	^5G	.....
			^3G	60456.0	$^4H'$	65589.1	$^5H'$	.....
			^1S	64942.8	$^2P'$	.....	$^3P'$	.....
			$^1P'$	60400.0	^2D	.....	^3D	.....
			^1D	64366.2	$^2F'$	65458.6	$^3F'$	.....
			$^1F'$	59528.2	^2G	67820.9	^3G	.....
			^1G	65235.8	$^2H'$	68582.3	$^3H'$	.....
$d^{n-2}f$	^2F	68054.0	.....	.....	.....	.....	.....	.....

TABLE II—*Continued*

Configuration	n=6, Cr^+		n=7, Mn^+		n=8, Fe^+		n=9, Co^+	
$d^{n-2}s$	^6D	0.0	^7S	0.0	^6D	0.0	$^5F'$	0.0
							$^5P'$	.....
	^4D	7527.5	^5S	9472.9	^4D	7955.2	$^3F'$	.....
							$^3P'$	.....
d^{n-1}.....	^6S	−12498.3	^5D	14324.5	$^4F'$	1872.6	$^3F'$	(−3500)
					$^4P'$	13474.3	$^3P'$	.....
$d^{n-3}s^2$	$^4F'$	.....	^5D	.....	^6S	23317.6	^5D	.....
$d^{n-2}p$	^6P	36135.6	^7P	38806.5	^6P	42658.3	$^5D'$	42028.3
	$^6D'$	37341.8	.....	.....	$^6D'$	38458.9	^5F	41847.4
	^6F	35255.1	.....	.....	^6F	41968.1	$^5G'$	43728.0
	^4P	36855.0	^5P	43370.4	^4P	46967.3	$^3D'$	.....
	$^4D'$	42287.9	.....	.....	$^4D'$	44446.8	^3F	.....
	^4F	39446.2	.....	.....	^4F	44232.5	$^3G'$	.....
$d^{n-3}s\,p^1$.....	$^6D'$	.....	^7P	.....	^8P	.....	^7P	.....
	^6F	.....	$^7D'$	.....	.....	.....	$^7D'$	.....
	$^6G'$	.....	^7F	.....	.....	.....	^7F	.....
	$^4D'$	.....	^5P	.....	^6P	.....	^5P	.....
	^4F	.....	$^5D'$	.....	.....	.....	$^5D'$	.....
	$^4G'$	.....	^5F	.....	.....	.....	^5F	.....
$d^{n-2}\cdot s$	^6D	.....	^7S	74558.4	^6D	.....	$^5F'$	.....
	^4D	.....	^5S	.....	^4D	.....	$^3F'$	.....
$d^{n-2}\cdot d$	^6S	.....	^7D	79568.4	^6S	.....	$^5P'$	.....
	$^6P'$	.....	.....	.....	$^6P'$	.....	^5D	.....
	^6D	.....	.....	.....	^6D	.....	$^5F'$	.....
	$^6F'$	.....	.....	.....	$^6F'$	.....	^5G	.....
	^6G	.....	.....	.....	^6G	.....	$^5H'$	.....
	^4S	.....	^5D	.....	^4S	.....	$^3P'$	.....
	$^4P'$	.....	.....	.....	$^4P'$	.....	^3D	.....
	^4D	.....	.....	.....	^4D	.....	$^3F'$	.....
	$^4F'$	.....	.....	.....	$^4F'$	.....	^3G	.....
	^4G	.....	.....	.....	^4G	.....	$^3H'$	.....
$d^{n-2}f$	.....	.....	.....	.....	.....	.....	.....	.....

TABLE II—*Continued*

Configuration	n=10, Ni^+		n=11, Cu^+		n=12, Zn^+	
$d^{n-2}s$	$^4F'$	0.0	^3D	0.0	^2S	0.0
	$^4P'$	16641.7	.....	.....	.....	.....
	$^2F'$	5156.2	^1D	4335.7	.....	.....
	$^2P'$	20676.5	.....	.....	.....	.....
d^{n-1}	^2D	(−8200)	^1S	−21925	.....	.....
	.....	.....	.....	.....	.....	.....
$d^{n-3}s^2$	$^4F'$	.....	$^3F'$	.....	^2D	62721.2
$d^{n-2}p$	$^4D'$	43164.0	^3P	44489.9	^2P	49353.7
	^4F	46163.2	$^3D'$	48912.5	.....	.....
	$^4G'$	45102.7	^3F	46802.1	.....	.....
	$^2D'$	49025.6	^1P	51667.1	.....	.....
	^2F	48686.2	$^1D'$	51424.3	.....	.....
	$^2G'$	46905.9	^1F	49991.3	.....	.....
$d^{n-3}s\,p$	$^6D'$	.....	$^5D'$	.....	$^4D'$	.....
	^6F	.....	^5F	.....	^4F	.....
	$^6G'$	.....	$^5G'$	.....	$^4G'$	.....
	$^4D'$	.....	$^3D'$	.....	$^2D'$	.....
	^4F	.....	^3F	.....	^2F	.....
	$^4G'$	.....	$^3G'$	.....	$^2G'$	.....
$d^{n-2}\cdot s$	$^4F'$	83404.4	^3D	86083.7	^2S	88435.8
	$^2F'$	85132.2	^1D	88435.0	.....	.....
$d^{n-2}\cdot d$	$^4P'$	.....	^3S	.....	^2D	96958.8
	^4D	.....	$^3P'$	.....	.....	.....
	$^4F'$	.....	^3D	.....	.....	.....
	^4G	.....	$^3F'$	.....	.....	.....
	$^4H'$	.....	^3G	.....	.....	.....
	$^2P'$	.....	^1S	.....	.....	.....
	^2D	.....	$^1P'$	.....	.....	.....
	$^2F'$	.....	^1D	.....	.....	.....
	^2G	.....	$^1F'$	.....	.....	.....
	$^2H'$	.....	^1G	.....	.....	.....
$d^{n-2}f$	.....	.....	.....	.....	^2F	117262.2

larities in arrangement of the various terms more apparent. Only the component of greatest inner-quantum number is tabulated. When the terms are "regular," this lies higher than the zero level, which corresponds to the smallest inner-quantum number. In a few of the spark spectra the lowest term has not yet been observed, but its position may be approximately found by means of series in the arc spectrum of the same element. These values are given in paren-

theses and in round numbers. Only the terms arising from those of highest multiplicity in the d^{n-2} or d^{n-1} configurations are tabulated, and the derivative terms arising from the P′ terms which accompany the F′ terms are omitted, because, where known, they give weaker lines. Even so, there are many blanks in the table, where terms remain to be found, and no attempt has been made to leave space for all the possible terms coming from $d^{n-2}\,s{\cdot}d$ or $d^{n-2}\,p^2$.

The assignment of the low terms to the various configurations follows Hund. That of the higher terms, in the cases of *Sc*, *Ti*, *Fe*, *Ni*, and *Cu*, is taken from the sources already listed. The remaining spectra have been reviewed by the writer for the present purpose.

There is no room for full details here; but it may be said that the principles that the strongest combinations occur between related terms having the same parent term in the next higher spectrum, and that the terms of a triad or pentad usually lie at nearly the same level, generally suffice to identify the principal terms with reasonable security. Series relations identify most of the high even terms with certainty. A few terms for which the assignment to the given configuration is doubtful are marked with colons in the table.

5. REMARKS ON SPECTRAL STRUCTURE

Many striking regularities are shown in this table. The orderly change in the multiplicities and types of the terms is a direct consequence of Hund's theory, as is also the fact that, among the terms of similar origin, those of the higher multiplicity are almost always at the lower level.

The levels corresponding to excited configurations of the atom $d^{n-2}\,s\,p$, $d^{n-2}\,s{\cdot}s$, $d^{n-2}\,s{\cdot}d$, rise steadily, compared with $d^{n-2}\,s^2$, as the atomic number increases; and the same is true of $d^{n-1}\,p$, $d^{n-1}{\cdot}s$, $d^{n-1}{\cdot}d$ relative to $d^{n-1}\,s$. These relations are illustrated in Figures 1 and 2, in which, to avoid confusion, each triad or pentad is represented by a single point at the mean level of the known terms belonging to it.

The lines connect the points representing those terms which are related, not merely as regards the electron configurations, but also with respect to the multiplicity, and are found in the same column in Tables I and II. Some of these series of terms are longer than others, for the lower multiplicities do not always appear. Gaps where no ob-

servational data are at present available are bridged by dotted lines. Exactly the same relations (Fig. 3) hold good among the spark spectra.

The general upward trend of these lines is simply explained on the orbital theory of the atom. On passing up a series of homologous configurations, successive 3d electrons are built into the atoms, leaving the other orbits unaltered. In the group of

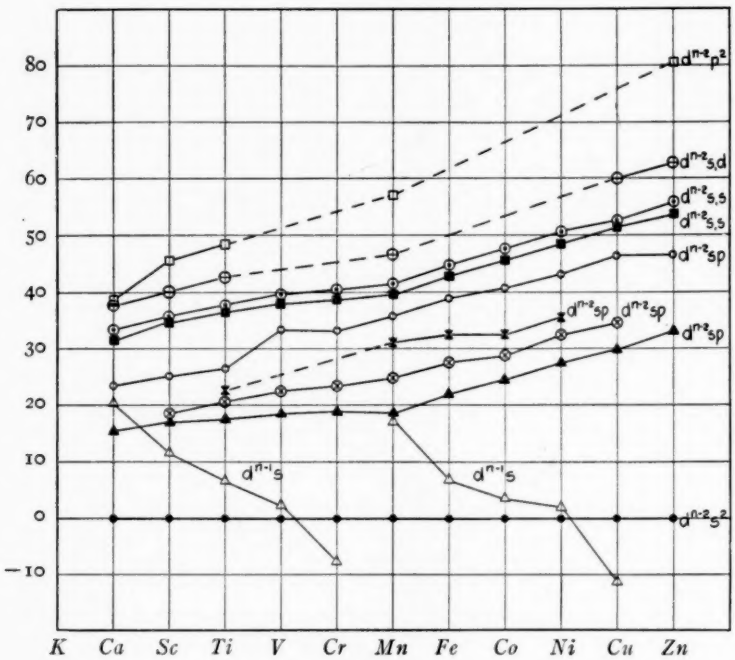

FIG. 1.—Energy levels relative to $d^{n-2}s^2$

configurations represented in Figure 2, for example, the only difference between the normal and excited states is that a single electron is shifted from a 4s to a 4p, 5s, or 5d orbit, and the difference of the spectroscopic terms represents the difference of the energy of binding of the electron to the atom in these orbits. For successive elements the nuclear charge increases. At a distance this increase is effectively neutralized by the influence of the additional 3d electrons; but for electrons such as are named above, all of which have orbits which at pericenter penetrate inside the 3d

orbits, the "screening" of the additional central charge by the 3d electrons is incomplete. Every addition of such an electron, therefore, increases the average force with which the electron now specially considered is bound to the atom, and the energy of binding, which is directly shown by the increase in the ionization potential (discussed in a following paper).[1] This increase of binding energy is greater for the 4s electron than for the others; hence the difference of the spectroscopic terms increases with the atomic number.

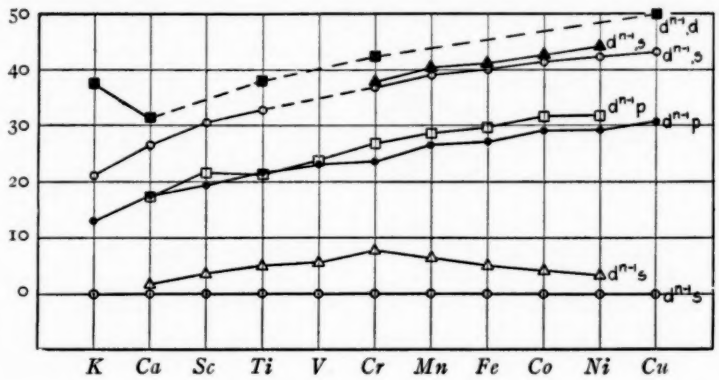

FIG. 2.—Energy levels relative to $d^{n-1}s$

This explanation, though conventional, is of course greatly oversimplified. What is really observed in the spectroscopic terms is the relative energy possessed by the atom as a whole, and not by any single electron in it, so that the "screening" should really take account of the combined influence of all the orbits. This is illustrated by the course of the differences between $d^{n-2}s^2$ and $d^{n-1}s$, or between $d^{n-2}s$ and d^{n-1} in the spark spectrum. Here the 3d electron appears to be bound with much more rapidly increasing energy than the 4s, until the shell of electrons is half-full in *Cr*, after which an abrupt change occurs in both the arc and spark spectra, and the energy differences nearly repeat themselves. Very similar relations appear in the second long period.[2] The break is associated with

[1] *Mt. Wilson Contr.*, No. 342; *Astrophysical Journal*, **66**, 1927.

[2] O. Laporte, *Journal of the Optical Society of America*, **13**, 1, 1926. A similar discontinuity has been noticed for the shell of p electrons by McLennan and McLay, *Philosophical Magazine*, **4**, 407, 1927.

the change from increasing to decreasing multiplicity, and the appearance of inverted terms. It is easily explained by the reversal of the direction of spin of the added electron, which is demanded by Pauli's exclusion principle when a shell is more than half completed.

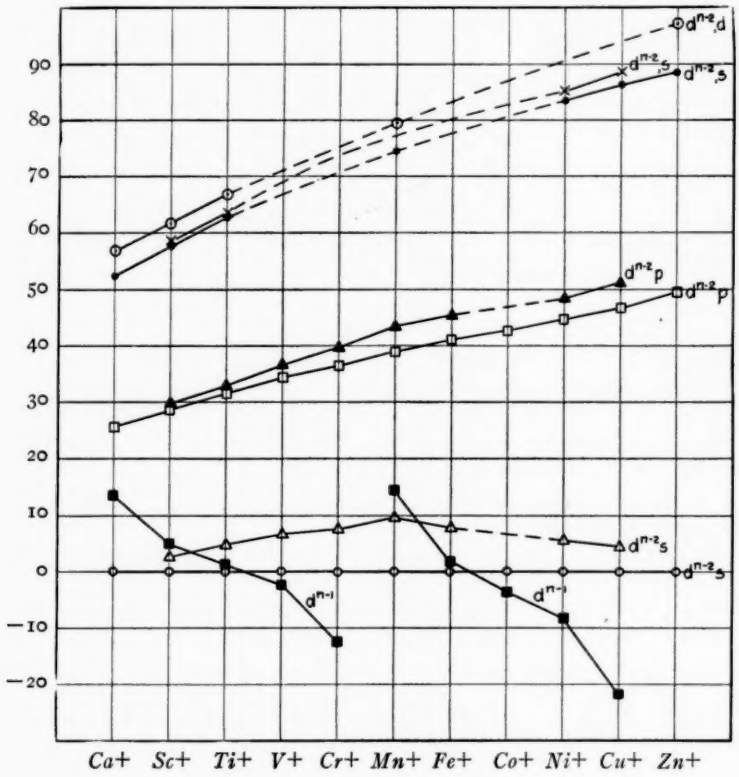

FIG. 3.—Energy levels relative to $d^{n-2}s$

Figures 1 and 2 bring out clearly many points of the spectral structure, some of which were previously puzzling. For example, the configuration $d^{n-2}sp$ gives rise in the arc spectra from *Sc* to *Cu* to two triads of the same multiplicity—doublets in *Sc*, triplets in *Ti*, and so on. In the spark spectra of the same elements, $d^{n-2}s$ gives rise to terms of the same name but different multiplicity, e.g., ^3D and ^1D in *Sc* II. It is evident that one of the arc triads, if the

p electron were removed, step by step, would give rise to a series having as its limit the spark term of higher multiplicity, and the other to a series with the limit of lower multiplicity; but it is hardly practicable from inspection of a single spectrum to tell which belongs to which limit.[1] Figure 1 solves the problem, making it quite clear that the higher-lying of the two triads belongs to the sequence which begins with the ^{1}P term in *Ca* and ends with the similar term in *Zn*, while the lower-lying sequence has no correlatives in these spectra. In the spark spectra the d^{n-1} s terms of higher multiplicity form a sequence beginning with ^{2}S in *Ca*, ^{3}D in *Sc*, and ending with ^{2}S in *Zn*, while those of lower multiplicity begin with ^{1}D in *Sc* and end with the similar term in *Cu*. It is now evident that the higher set of triads must have the term of higher multiplicity as limit, which agrees with the fact that they give the stronger combinations. There are two other sequences of triads of origin d^{n-2} s p and of multiplicity higher and lower than those just considered, for example, quintets and singlets in *Ti* (the two being triplets). There can be no question about assigning these to the limits of high and low multiplicity, respectively, and it is now noteworthy that the terms of greater multiplicity always lie lower than those of smaller multiplicity arising from the same limit. This difference of level is much greater in the case of the terms with the limit of high multiplicity. Why this should be so is an excellent problem for the theorists.

6. TABLES OF HOMOLOGOUS LINES

The principal lines which result from combinations of the terms given in Tables I and II are listed in Tables III and IV. Each of the wide columns of the table gives data for a series of homologous lines, for which the electron jump is the same and the multiplicities are related as described above. Only the leading lines of the multiplets are given. The remainder may be found in most cases in the writer's "List of Ultimate and Penultimate Lines."[2] The letter *i* denotes that the predicted multiplet is in the infra-red. The intensities and temperature classes are taken from King's lists when available. Values derived from other sources are given in parentheses. The scale of

[1] Russell and Meggers, *Scientific Papers of the Bureau of Standards*, No. 558.

[2] *Mt. Wilson Contr.*, No. 286; *Astrophysical Journal*, **61**, 223–283, 1925.

intensities is not homogeneous throughout, nor even always for a single element. In certain cases, as in the combinations of a triad and a pentad of terms or in groups of intercombinations, only a few of the strongest multiplets are selected. It should be recalled once more that the list is very far from exhaustive, for only those terms

TABLE III

HOMOLOGOUS LINES IN ARC SPECTRA

ELEMENT	$d^{n-1}s^2-d^{n-1}sp$								
	Upper Triad			Lower Triad			Intersystem		
K.....	.....	.....	.....	.....	.....		.....	.....	.....
Ca.....	$^1S-^1P$	4226.7	500 I	.....	.....		$^3S-^3P$	6572.8	8 I A
Sc.....	$^2D-^2F$	3911.8	100 II	4779.4	20 I A		$^2D-^4F$	6413.4	50 I A
	$^2D'$	4023.7	100 II	6305.7	400 I A		$^4D'$	6259.0	100 I A
	^2P	4082.4	40 I	5349.7	15 II A		.....	.....	.....
Ti.....	$^3F'-^3G'$	3371.4	80 II	4681.9	30 I		$^3F'-^5G'$	6296.7	2 I A
	^3F	3998.6	100 II	5210.4	40 I		$^5D'$	5460.5	4 I A
	$^3D'$	3958.2	80 II	5064.6	25 I		$^5G'$	4112.7	20 II
V.....	$^4F'-^4G'$	3185.4	40 II	4594.1	60 I		$^4F'-^6D'$	5632.5	1 II A
	^4F	3066.4	125 II	4352.9	50 I		.....	.....	.....
	$^4D'$	2923.6	70 II	4881.5	50 I		.....	.....	.....
Cr.....	$^5D-^5F$	3021.6	100 II	4351.8	60 I		$^5D-^7D'$	5122.1	4 I
	$^5D'$	2986.5	100 II	3919.2	35 II		^7P	5123.5	6 I
	^5P	3053.9	125 II	4646.2	40 I		.....	.....	.....
Mn.....	$^6S-^6P$	2794.8	500 IV	4030.8	200 I		$^6S-^8P$	5394.7	10 I A
							^4P	3224.8	4 II
Fe.....	$^5D-^5F$	2483.3	60 II	3719.9	250 I		$^5D-^7F$	4427.3	10 I
	$^5D'$	2522.9	40 II	3859.9	300 I		$^7D'$	5110.4	10 I
	^5P	2719.0	60 II	3440.6	150 I		^7P	4216.2	8 I
							^3P	2981.4	20 I
Co.....	$^4F'-^4G'$	2407.3	(30 R)	3465.8	100 II		$^4F'-^6G'$	3909.9	15 I
	^4F	2425.0	(30 R)	3526.9	100 II		^6F	4190.7	20 I
	$^4D'$	2521.4	(30 R)	3412.6	80 II		$^6G'$	3237.0	8 II
Ni.....	$^3F'-^3G'$	2320.0	(5 R)	3232.9	25 II		$^3F'-^5G'$	3624.7	15 II
	^3F	2311.0	(3 R)	3031.9	10 II		$^5D'$	3749.0	8 I
	$^3D'$	.....	.....	2984.1	12 II		^1F	2991.1	4 II
Cu.....	$^2D-^2F$	2230.1	(6 R)	2961.2	(6)		$^2D-^4F$	3337.9	(6)
	$^2D'$	2130.8	(1)	2824.4	(8)		$^4D'$	3094.0	(6)
	^2P	2138.5	(1 R)	2883.0	(4)		^4P	3594.0	(2)
Zn.....	$^1S-^1P$	2138.6	(8 R)	.....	.....		$^1S-^3P$	3075.9	(8 R)

TABLE III—*Continued*

Element	$d^{n-1}s-d^{n-1}p$								
	High Multiplicity			Low Multiplicity			Intersystem		
K	$^2S-^2P$	7664.9	(10 R)	.....	.....	.....	.....	.....	.....
Ca	$^3D-^3F$	6439.1	150 II	$^1D-^1F$	5349.5	25 III	$^1D-^3F$	7202.2	3 II
	$^3D'$	5588.7	80 III	$^1D'$	7148.1	10 II	.....	.....	.....
	^3P	5270.3	60 III	^1P	6717.7	30 III	$^3D-^1D'$	6449.8	50 II
Sc	$^4F'-^4G'$	5671.8	200 II	$^2F'-^2G'$	5520.5	100 III	$^2F'-^4G'$	.....	.....
	^4F	5081.6	125 II	^2F	5482.0	100 III	.....	.....	.....
	$^4D'$	4743.8	40 III	$^2D'$	5356.1	60 III	$^4F'-^2G'$	.....	.....
Ti	$^5F'-^5G'$	4981.8	60 II	$^3F'-^3G'$	6258.7	50 II	$^3F'-^5G'$	6666.6	(2)
	^5F	4533.3	80 II	^3F	6556.1	25 III	.....	.....	.....
	$^5D'$	4305.9	60 II	$^3D'$	5512.5	25 II	$^5F'-^3G'$	4781.7	6 III A
V	$^6D-^6F$	4379.2	150 II	$^4D-^4F$	5727.0	60 I	$^4D-^6F$	6128.3	2 III A
	$^6D'$	4111.8	100 I	$^4D'$	5627.6	30 I	.....	.....	.....
	^6P	4460.3	50 I	^4P	6090.2	50 I	$^6D-^4F$	4209.9	20 I
Cr	$^7S-^7P$	4254.3	500 II	$^5S-^5P$	5208.4	300 II	$^5S-^7P$	6330.1	25 I A
							$^7S-^5P$	3732.0	12 I
Mn	$^6D-^6F$	3806.9	20 I	$^4D-^4F$	4762.4	30 III	$^4D-^6F$	4965.9	3 III
	$^6D'$	4041.4	50 I	$^4D'$	4451.6	15 II	.....	.....	.....
	^6P	3577.9	40 II	^4P	4235.3	8 I	$^6D-^4F$	3670.5	3 III
Fe	$^5F'-^5G'$	3581.2	250 I	$^3F'-^3G'$	4271.8	35 II	$^3F'-^5G'$	4383.5	45 II
	^5F	3734.9	300 II	^3F	4045.8	60 II	.....	.....	.....
	$^5D'$	3820.4	250 II	$^3D'$	3815.8	100 II	$^5F'-^3G'$	3513.8	30 II
Co	$^4F'-^4G'$	3453.5	200 II	$^2F'-^2G'$	3845.5	60 II	$^2F'-^4G'$	3995.3	60 II
	^4F	3405.1	150 II	^2F	3569.3	80 II	.....	.....	.....
	$^4D'$	3502.3	100 II	$^2D'$	3489.4	60 II	$^4F'-^2G'$	3412.3	80 II
Ni	$^3D-^3F$	3414.8	150 II	$^1D-^1F$	3619.4	150 II	$^1D-^3F$	3858.3	40 II
	$^3D'$	3393.0	100 II	$^1D'$	3566.4	100 II	.....	.....	.....
	^3P	3524.5	200 II	^1P	3380.6	80 II	$^3D-^1F$	3243.1	25 I
Cu	$^2S-^2P$	3247.5	(10 R)	.....	.....	.....	.....	.....	.....
Zn	.....	.....	.....	.....	.....	.....	.....	.....	.....

TABLE III—*Continued*

Element	$d^{n-1}s-d^{n-2}sp$					
	High Multiplicity			Low Multiplicity		
K	.....	.....	.....	.....	.....	.....
Ca	$^3D-^3P$	19771.1	.....	$^1D-^1P$	*i*	.....
Sc	$^4F'-^4F$	*i*	.....	$^2F'-^2F$	*i*	.....
	$^4D'$	*i*	.....	$^2D'$	*i*	.....
	^4P	*i*	.....	^2P	*i*	.....
Ti	$^5F'-^5G'$	*i*	.....	$^3F'-^3G'$	5474.3	6 II
	^5F	9638.3	(2)	^3F	7344.7	4 IV
	$^5D'$	8435.6	(5)	$^3D'$	7209.4	20 III
V	$^6D-^6G'$	.....	.....	$^4D-^4G'$	.....	.....
	^6F	6150.1	15 I	^4F	6753.0	5 III A
	$^6D'$	6243.1	30 I	$^4D'$	8116.8	(5)
Cr	$^7S-^7F$	.....	.....	$^5S-^5F$	.....	.....
	$^7D'$	3615.7	4 II A	$^5D'$	3870.3	3 III
	^7P	3578.7	200 II	^5P	4496.9	25 I
Mn	$^6D-^6P$	12899.7	(8)	$^4D-^4P$	12975.9	(4)
	$^6D-^6P$	5341.1	20 III A	.....	.....	.....
Fe	$^5F'-^5F$	5012.1	12 I	$^3F'-^3F$	5171.6	20 II
	$^5D'$	5269.5	60 I	$^3D'$	5167.5	40 II
	^5P			^3P	4765.5	(1)
Co	$^4F'-^4G'$	3941.7	20 II	$^2F'-^2G'$	4121.4	60 II
	^4F	4020.9	20 I	^2F	4092.4	25 I
	$^4D'$	3873.1	60 II	$^2D'$	3842.1	30 II
Ni	$^3D-^3G'$	3234.7	10 II	$^1D-^1G'$	.....	.....
	^3F	3050.8	100 II	^1F	3101.9	40 II
	$^3D'$	3002.5	100 II	$^1D'$	3012.0	75 II
Cu	$^2S-^2F$	.....	.....	.....	.....	.....
	$^2D'$	2165.1	(1 R)	.....	.....	.....
	^2P	2179.0	(1 R)	.....	.....	.....
Zn	.....	.....	.....	.....	.....	.....

TABLE III—*Continued*

Element	$d^{n-2}s^2-d^{n-1}p$ (Double Electron Jump)					
				Intersystem		
K						
Ca	$^1S-{}^1P$	2721.7		$^1S-{}^3F$		
				$^3D'$	2617.6	(3)
				^3P	2541.4	(0)
Sc	$^2D-{}^2G'$	3039.8	(0) III A	$^2D-{}^4G'$	3455.9	(2) (II A)
	^2F	3019.3	10 II	^4F	3213.8	(0) (III A)
	$^2D'$	2980.7	(6)	$^4D'$	3073.3	(1) (III A)
Ti	$^3F'-{}^3G'$	3653.5	100 I	$^3F'-{}^5G'$	3788.8	2 III A
	^3F	3752.9	80 I	^5F	3506.6	8 I
	$^3D'$	3385.9	40 II	$^5D'$	3377.5	20 I
V	$^4F'-{}^4F$	3902.3	50 I	$^4F'-{}^6F$	4070.8	4 II
	$^4D'$	3855.9	60 I	$^6D'$	3817.9	8 I A
	^4P	4029.9	2 III A	^6P		
Cr	$^5D-{}^5P$	5409.8	100 I	$^5D-{}^7P$	6630.0	4 I A
Mn	$^6S-{}^6F$	2296.9	(3)	$^6S-{}^4F$		
	$^6D'$	2384.0	(2)	$^4D'$	2184.8	(1)
	^6P	2221.6	(9)	^4P		
Fe	$^5D-{}^5G'$	2874.2	10 I	$^5D-{}^3G'$	2825.7	6 II
	^5F	2966.9	125 II	^3F	2690.1	2 III
	$^5D'$	3020.6	200 I	$^3D'$	2618.7	2 III
Co	$^4F'-{}^4G'$	3082.6	12 II	$^4F'-{}^2G'$	2989.6	15 II
	^4F	3044.0	30 II	^2F	2820.0	(2)
	$^4D'$	3121.4	10 II	$^2D'$	2833.9	(1)
Ni	$^3F'-{}^3F$	3391.1	50 II	$^3F'-{}^1F$	3366.2	20 II
	$^3D'$	3369.6	80 II	$^1D'$	3320.3	20 II
	^3P	3670.4	20 II	^1P	3249.4	6 I
Cu	$^2D-{}^2P$	5105.6	(8 R)			
Zn						

TABLE III—*Continued*

Element	$d^{n-2}sp-d^{n-2}s\cdot s$					
	High Multiplicity			Low Multiplicity		
K						
Ca	$^3P-^3S$	6162.2	150 II			
Sc	$^4F-^4D$	5392.1	30 III	$^2F-^2D$	6819.5	(20)
	$^4D'-^4D$	5446.2	20 III	$^2D'-^2D$	5068.9	2 III
	$^4P-^4D$	6250.0	15 IV	$^2P-^2D$	5919.2	tr IV A
Ti	$^5G'-^5F'$	5025.6	18 III	$^3G'-^3F'$	6215.2	20 III
	$^5F-^5F'$	5224.3	15 III	$^3F-^3F'$	5477.7	8 III
	$^5D'-^5F'$	5662.2	12 III	$^3D'-^3F'$	5648.6	5 IV
V	$^6G'-^6F'$	4807.5	25 III	$^4G'-^4F'$	5784.4	5 III
	$^6F-^6F'$	5193.0	7 III	$^4F-^4F'$	6218.3	3 IV
	$^6D'-^6F'$	5128.5	7 III	$^4D'-^4F'$	5385.1	3 III
Cr	$^7F-^7D$	4718.5	20 III	$^5F-^5D$	5698.3	20 III
	$^7D'-^7D$	5225.0	25 III	$^5D'-^5D$	6661.1	12 IV
	$^7P-^7D$	5255.1	15 IV	$^5P-^5D$	5261.8	6 IV
Mn	$^8P-^8S$	4823.5	50 I	$^6P-^6S$	6021.8	50 III
Fe	$^7F-^7D$	4957.6	60 III	$^5F-^5D$	5615.7	50 IV
	$^7D'-^7D$	4260.5	35 III	$^5D'-^5D$	5324.2	30 IV
	$^7P-^7D$	5232.9	40 III	$^5P-^5D$	6400.0	25 III
Co	$^6G'-^6F'$	4867.9	25 II	$^4G'-^4F'$	5352.0	20 III
	$^6F-^6F'$	4531.0	30 III	$^4F-^4F'$	5212.7	25 III
	$^6D'-^6F'$	4749.7	10 III	$^4D'-^4F'$	5484.0	10 V
Ni	$^5G'-^5F'$	4714.4	25 II	$^3G'-^3F'$	5115.4	8 V
	$^5F-^5F'$	5017.6	10 III?	$^3F-^3F'$	5715.1	6 V
	$^5D'-^5F'$	4401.6	30 III	$^3D'-^3F'$	5614.8	5 V
Cu	$^4F-^4D$	4651.1	(8)	$^2F-^2D$	5076.2	(3u)
	$^4D'-^4D$	5292.5	(4)	$^2D'-^2D$	5535.8	(3u)
	$^4P-^4D$	4275.1	(6)	$^2P-^2D$		
Zn	$^3P-^3S$	4810.5	(10 R)			

TABLE III—*Continued*

Element	$d^{n-1}p-d^{n-1}\cdot s$					
	High Multiplicity			Low Multiplicity		
K	$^2P-^2S$	12523.0	.....	.....	.....	.....
Ca	$^3F-^3D$	9250.8:	(2)	$^1F-^1D$	.....	.....
	$^3D'-^3D$	11840 :	(5)	$^1D'-^1D$	.....	.....
	$^3P-^3D$	.....	.....	$^1P-^1D$	.....	.....
Sc	$^4G'-^4F'$	7821.6	(6)	$^2G'-^2F'$	.....	.....
	$^4F-^4F'$	*i*	.....	$^2F-^2F'$	.....	.....
	$^4D'-^4F'$	*i*	.....	$^2D'-^2F'$	.....	.....
Ti	$^5G'-^5F'$	7996.5	(3)	$^3G'-^3F'$	.....	.....
	$^5F-^5F'$	*i*	.....	$^3F-^3F'$	.....	.....
	$^5D'-^5F'$	*i*	.....	$^3D'-^3F'$	.....	.....
V	$^6F-^6D$	*i*	.....	$^4F-^4D$	.....	.....
	$^6D'-^6D$	*i*	.....	$^4D'-^4D$	.....	.....
	$^6P-^6D$	*i*	.....	$^4P-^4D$	.....	.....
Cr	$^7P-^7S$	7462.3	(10)	$^5P-^5S$	9009.9	(6)
Mn	$^6F-^6D$	7764.8	(5)	$^4F-^4D$	7680.2	(5)
	$^6D'-^6D$	6942.6	(5)	$^4D'-^4D$	8654.6	(2)
	$^6P-^6D$	8929.7	(1)	$^4P-^4D$	*i*	.....
Fe	$^5G'-^5F'$	8220.4	(7)	$^3G'-^3F'$	7945.9	(7)
	$^5F-^5F'$	7511.1	(9)	$^3F-^3F'$	8866.9	(3)
	$^5D'-^5F'$	7187.4	5 V	$^3D'-^3F'$	*i*	.....
Co	$^4G'-^4F'$	8094.0	8 III	$^2G'-^2F'$	7027.9	6 V
	$^4F-^4F'$	8372.8	(10)	$^2F-^2F'$	7113.7	5 V
	$^4D'-^4F'$	7838.2	3 V	$^2D'-^2F'$	8022.2	(7)
Ni	$^3F-^3D$	7617.0	5 III	$^1F-^1D$	7555.7	5 III
	$^3D'-^3D$	7727.7	3 IV	$^1D'-^1D$	7797.7	3 V
	$^3P-^3D$	7122.3	100 IV	$^1P-^1D$	8862.6	(4)
Cu	$^2P-^2S$	8092.7	(10)	.....	.....	.....
Zn	.....	.....	.....	.....	.....	.....

TABLE III—*Continued*

Element	$d^{n-2}sp-d^{n-2}s\cdot d$			$d^{n-2}sp-d^{n-2}p^2$		
K	.....	.....	.....	.....	.....	.....
Ca	$^3P-^3D$	4454.8	80 I	$^3P-^3P'$	4302.5	60 I
Sc	$^4F-^4G$	4165.2	12 III	$^4F-^4F'$	3435.6	5 III A
	$^4D'-^4F'$	4087.2	8 III	$^4D'-^4F'$	3457.5	3 III A
	$^4P-^4D$	4709.3	5 III	.....	.....	.....
Ti	$^5G'-^5H'$	3882.9	20n III?	$^5G'-^5G$	3226.1	12 III
	$^5F-^5G$	4030.5	25n III	$^5G'-^5F'$	3123.8	20n IV
	$^5D'-^5F'$	4058.2	7 IV	$^5F-^5D$	3141.7	10 IV
V	$^6G'-^6H'$	.....	.....	.....	.....	.....
	$^6F-^6G$	.....	.....	.....	.....	.....
	$^6D'-^6F'$	.....	.....	.....	.....	.....
Cr	$^7F-^7G$	.....	.....	.....	.....	.....
	$^7D'-^7F'$	.....	.....	.....	.....	.....
	$^7P-^7D$	.....	.....	.....	.....	.....
Mn	$^8P-^8D$	3569.5	60 III	$^8P-^8P'$	2584.3	(4)
Fe	$^7F-^7G$	.....	.....	.....	.....	.....
	$^7D'-^7F'$	.....	.....	.....	.....	.....
	$^7P-^7D$	.....	.....	.....	.....	.....
Co	$^6G'-^6H'$	.....	.....	.....	.....	.....
	$^6F-^6G$	.....	.....	.....	.....	.....
	$^6D'-^6F'$	.....	.....	.....	.....	.....
Ni	$^5G'-^5H'$	.....	.....	.....	.....	.....
	$^5F-^5G$					
	$^5D'-^5F'$	.....	.....	.....	.....	.....
Cu	$^4F-^4G$	3308.0	(8)	.....	.....	.....
	$^4D'-^4F'$	3599.1	(6)	.....	.....	.....
	$^4P-^4D$	3099.9	(4)	.....	.....	.....
Zn	$^3P-^3D$	3344.9	(10 R)	$^3P-^3P'$	2096.9	(2)

TABLE IV

RELATED LINES IN SPARK SPECTRA

ELEMENT	$d^{n-1}s-d^{n-1}p$									
	High Multiplicity				Low Multiplicity				Intersystem			
Ca^+...	$^2S-^2P$	3933.7	400	II	.....	.....	.....		.....	.....	.....	
Sc^+....	$^3D-^3F$	3613.8	30	II	$^1D-^1F$	3353.7	10	III	$^1D-^3F$	4014.5	5	IV
	$^3D'$	3572.5	20	II	$^1D'$	4246.8	75	III				
	^3P	3372.1	12	III	^1P	3535.7	6	III	$^3D-^1P$	3251.3	1	IV
Ti^+...	$^4F'-^4G'$	3349.4	40	II	$^2F'-^2G'$	3349.0	20	III	$^2F'-^4D'$	3596.0	10	V
	^4F	3234.5	60	III	^2F	3759.3	40	IV				
	$^4D'$	3088.0	60	III	$^2D'$	3685.2	40	IV	$^4F'-^2D'$	3143.8	10	IV
V^+....	$^5F'-^5G'$	3093.1	50	III	$^3F'-^3G'$	3276.1	20	V	$^3F'-^5D'$	3517.3	12	V
	^5F	2924.0	30	IV	^3F	3190.7	15	V				
	$^5D'$	2908.8	30	IV	$^3D'$	3593.3	12	V	$^5F'-^3D'$	2930.8	15	IV
Cr^+...	$^6D-^6F$	2835.6	40	V	$^4D-^4F$	3132.1	20	V	$^4D-^6P$	3511.8	6	V
	$^6D'$	2677.1	25	V	$^4D'$	2876.0	10	V				
	^6P	2766.6	30	V	^4P	3408.8	15	V	$^6D-^4P$	2698.4	10	V
Mn^+...	$^7S-^7P$	2576.2	(10	R)	$^5S-^5P$	2949.2	30	IV	$^5S-^7P$	3439.0	6	V
									$^7S-^5P$	2305.0	(2)	
Fe^+...	$^6D-^6F$	2382.0	(10)		$^4D-^4F$	2755.7	(9)		$^4D-^6F$	2926.6	(6)	
	$^6D'$	2599.4	(10)		$^4D'$	2739.6	(10)					
	^6P	2343.5	(7)		^4P	2562.5	(9)		$^6D-^4F$	2260.1	(3)	
Co^+...	$^5F'-^5G'$	2286.2	(100)		$^3F'-^3G'$	.....	.....		$^3F'-^5G'$	.....	.....	
	^5F	2388.9	(100)		^3F	.....	.....		.....	.....	.....	
	$^5D'$	2378.6	(100)		$^3D'$	.....	.....		$^5F'-^3G'$	.....	.....	
Ni^+...	$^4F'-^4G'$	2216.5	(100 | R)	$^2F'-^2G'$	2394.5	(50 | R)	$^2F'-^4G'$	2510.9	(30)	
	^4F	2165.6	(40 | R)	^2F	2296.6	(30 | R)				
	$^4D'$	2316.0	(80 | R)	$^2D'$	2278.8	(30 | R)	$^4F'-^2G'$	2131.3	(3)	
Cu^+...	$^3D-^3F$	2136.0	(10)		$^1D-^1F$	2189.6	(6)		$^1D-^3F$	2369.9	(6)	
	$^3D'$	2043.8	(8)		$^1D'$	2123.0	(5)					
	^3P	2247.0	(10)		^1P	2112.1	(5)		$^3D-^1F$	1999.7	(7)	
Zn^+...	$^2S-^2P$	2061.9	.....		.....	.....	.....		.....	.....	.....	

TABLE IV—*Continued*

Element	$d^{n-1}-d^{n-2}p$			$d^{n-2}p-d^{n-2}s$			$d^{n-2}p-d^{n-2}d$		
Ca^+...	$^2D-^2P$	8542.2	(10) V	$^2P-^2S$	3736.9	12 V	$^2P-^2D$	3179.3	15 V
Sc^+....	$^3F'-^3F$	4374.5	60 III	$^3F-^3D$	3343.3	1 III A	$^3F-^3G$	3065.1	(30)
	$^3D'$	4314.1	100 III	$^3D'-^3D$	3379.4	(3)	$^3D'-^3F'$	2826.7	(10)
	^3P	.....	.....	$^3P-^3D$	.....	.....	$^3P-^3D$	3312.7	(5)
Ti^+...	$^4F'-^4G'$	3444.3	15 III	$^4G'-^4F'$	3090.0	(2n)	$^4G'-^4H'$	2828.2	(7) V
	^4F	3322.9	20 III	$^4F-^4F'$	3194.5	(1)	$^4F-^4G$	2945.5	(5)
	$^4D'$	3168.5	30 III	$^4D'-^4F'$	3351.7	(1)	$^4D'-^4F'$	2752.9	(2)
V^+....	$^5D-^5G'$	.....	.....	$^5G'-^5F'$	.....	.....	.....	.....	.....
	^5F	2700.9	20 V	$^5F-^5F'$	.....	.....	.....	.....	.....
	$^5D'$	2688.0	35 V	$^5D'-^5F'$	.....	.....	.....	.....	.....
Cr^+...	$^6S-^6F$	.....	.....	$^6F-^6D$	.....	.....	.....	.....	.....
	$^6D'$	.....	.....	$^6D'-^6D$	.....	.....	.....	.....	.....
	^6P	2055.6	(5u)	$^6P-^6D$	.....	.....	.....	.....	.....
Mn^+...	$^5D-^5P$	3442.0	30 V	$^7P-^7S$	2796.2	(2)	$^7P-^7D$	2452.5	(10)
Fe^+...	$^4F'-^4F$	2360.0	(5)	$^6F-^6D$	.....	.....	.....	.....	.....
	$^4D'$	2348.1	(6)	$^6D'-^6D$	.....	.....	.....	.....	.....
	^4P	.....	.....	$^6P-^6D$	.....	.....	.....	.....	.....
Co^+...	$^3F'-^3G'$	.....	.....	$^5G'-^5F'$	.....	.....	.....	.....	.....
	^3F	.....	.....	$^5F-^5F'$	.....	.....	.....	.....	.....
	$^3D'$	.....	.....	$^5D'-^5F'$	.....	.....	.....	.....	.....
Ni^+...	$^2D-^2G'$	.....	.....	$^4G'-^4F'$	2610.1	(25u)	.....	.....	.....
	^2F	.....	.....	$^4F-^4F'$	2684.4	(20u)	.....	.....	.....
	$^2D'$	.....	.....	$^4D'-^4F'$	2484.3	(10u)	.....	.....	.....
Cu^+...	$^1S-^1P$	1358.8	(12)	$^3F-^3D$	2545.0	(10)	.....	.....	.....
				$^3D'-^3D$	2689.5	(7)	.....	.....	.....
				$^3P-^3D$	2403.5	(4)	.....	.....	.....
Zn^+...	.....	.....	.....	$^2P-^2S$	2502.0	(7)	$^2P-^2D$	2102.2	.....

which are derived from the lowest of the numerous metastable terms in the d^{n-1} or d^{n-2} configurations of the singly or doubly ionized atom have been considered at all. A comparison of the lines resulting from other terms will only be practicable in detail when some of the spectra have been more completely analyzed. Even in the limited part of the spectrum here considered many gaps remain to be filled, and other sets of related lines are not tabulated because our present knowledge of them is fragmentary.

Many relations between the different spectra are now conspicuous. The most general is the tendency of the stronger lines to draw

away into the ultra violet as the atomic number increases. These lines arise from transitions from the lower configurations including only 3d and 4s electrons to the middle configurations including a 4p electron, and the shift of the lines toward greater wave-numbers is the physical reality corresponding to the upward trend of the lines representing the middle configurations in Figures 1–3. It is therefore a direct result of the steady increase in the ionization potentials, and, by itself, provides sufficient qualitative evidence for such an increase —which may perhaps prove of value in the case of the rare earths. For the electron jump from 4p to 5s, the additional energy of binding in the neutral atoms is nearly the same for the two states, and the corresponding arc lines remain in the same region of the spectrum. Some of these transitions, for example that from the upper d^{n-2} s p triad to the d^{n-2} s·s terms of the same multiplicity, give lines which lie in the infra red, and are therefore known only for the few elements which have been investigated in this region.

For certain elements in the latter part of the first long period, notably for *As*, the two groups of lines corresponding to those just discussed have withdrawn completely into the ultra violet and the infra red, and the visible spectrum is completely empty.

The transition 4p – 4d gives terms which work slowly toward the violet, while that from (4s)(4p) to $(4p)^2$ gives, as might be expected, a very rapid shift to the shorter wave-lengths.

The transition d^{n-1} s – d^{n-2} s p, in which the electron jump is from 4p to 3d, gives lines shifting very rapidly to the violet, jumping back between *Cr* and *Mn*, and then going to the violet again, while for d^{n-2} s^2 – d^{n-1}p, which involves a double electron jump, the shift is toward the red, broken by a similar discontinuity. These are obvious consequences of the peculiar behavior of the relative levels discussed in the last section.

The individual sequences are noteworthy. Those which correspond to a transition 4s – 4p (d^{n-2} s^2 – d^{n-2}s p or d^{n-1} s – d^{n-1} p) include almost all the strongest lines in all the spectra.

The strongest multiplets in the sequence d^{n-2} s^2 – d^{n-2} s p have been tabulated by Gibbs and White,[1] who have pointed out the re-

[1] *Physical Review*, **29**, 661, 1927.

markably simple relations that exist between similar groups in spectra of several successive degrees of ionization.

In the first case, the transitions to the upper triad, which has the limits of higher multiplicity, give stronger lines than those to the lower triad, as far as *Mn*. Beyond this the lines of the first sequence get so far into the ultra violet that they are at an observational disadvantage. It would be of much interest to investigate, preferably by absorption observations, whether they actually continue to be the stronger. The transition $d^{n-1}\,s - d^{n-1}\,p$ gives stronger lines than that to the lower triad, except in *Mn* where the lower level involved lies unusually high.

The 3d − 4p jump ($d^{n-1}\,s - d^{n-2}\,s\,p$) gives fainter lines than those previously mentioned. The double electron jump ($d^{n-2}\,s^2 - d^{n-1}\,p$) produces surprisingly strong lines. In both these cases the low term and the triad with which it combines are often out of step, so to speak, and one or more of the transitions involves a change of more than one unit in the apparent azimuthal quantum number L (which is 0 for an S term, 1 for a P, and so on). Many of the transitions for which $\Delta L = 2$ give observable lines, some of them of considerable strength.

The intersystem combinations between terms of the same origin but different multiplicity are of considerable interest. In these lists the multiplets containing the strongest lines have been tabulated. The general increase in the intensity of the intercombinations with increasing atomic number is obvious, and, as is well known, may be attributed to the same cause as the increase in multiplet separations. The sequence $d^{n-2}\,s^2 - d^{n-2}\,s\,p$, beginning with *Ca* λ 6572, contains a remarkable number of the lines which are greatly strengthened in sun-spots. In the sequence $d^{n-1}\,s - d^{n-1}\,p$ the intercombinations are remarkably strong, culminating in the great iron line λ 4383.

The *raies ultimes* and resonance lines of these elements, as given by Laporte and Meggers,[1] are shown in Table V.

For the spark spectra the *raies ultimes* and resonance lines are identical, and arise in all instances from the transition $d^{n-2}\cdot s - d^{n-2}\cdot p$. In the arc spectra the resonance lines are intersystem combinations of origin $d^{n-2}\,s^2 - d^{n-2}\,s\,p$, and are of considerably longer wave-

[1] *Journal of the Optical Society of America*, **11**, 461, 1925, with unpublished corrections by Meggers. The resonance lines for *Co* and *Ni* are added from later work.

length than the *raies ultimes*, except for *K* and *Cr*, where they are identical with the latter and come from $d^{n-1}s-d^{n-1}p$. The *raies ultimes* come from $d^{n-2}s^2-d^{n-2}sp$ in most of the other spectra. The fact that they shift from the upper to the lower triad with increasing atomic number may be largely or entirely due to observational preference for lines in the near, rather than the far, ultra violet. The persistence of the $^4F'-{}^4G'$ group as well as the $^2D-{}^2F$ in *Sc* is an

TABLE V

Element	Raies Ultimes				Resonance Lines	
	Arc		Spark		Arc	
	λ	Origin	λ	Origin	λ	Origin
K	7664	2	.....	.....	7664	2
Ca	4226	1*a*	3933	4	6572	1*c*
Sc	3911	1*a*	3613	4	6413	1*c*
Ti	3653	3	3349	4	6295	1*c*
V	3185	1*a*	3093	4	5632	1*c*
Cr	4254	2	2835	4	4254	2
Mn	4030	1*b*	2576	4	5394	1*c*
Fe	3719	1*b*	2382	4	5166	1*c*
Co	3453	2	2388	4	4134	1*c*
Ni	3414	2	2416	4	3624	1*c*

Under "Origin" 1*a* denotes $d^{n-2}s^2-d^{n-2}sp$ (high triad)
1*b* denotes $d^{n-2}s^2-d^{n-2}sp$ (low triad)
1*c* denotes $d^{n-2}s^2-d^{n-2}sp$ (intersystem)
2 denotes $d^{n-1}s-d^{n-1}p$
3 denotes $d^{n-2}s^2-d^{n-1}p$
4 denotes $d^{n-2}s-d^{n-2}p$

example of the advantage of high *L* values discussed by Meggers.[1] The most remarkable case is *Ti*, in which the *raie ultime* involves a double electron jump. There is here no doubt about the correctness of the assignment of the electron configuration, for the intensities of the combinations are decisive. It is possible, however, that the $^3F'-{}^3G'$ line at λ 3371.4 may be actually as sensitive. The matter deserves further study.

The transition $d^{n-2}sp-d^{n-2}s\cdot s$ (4p–5s) gives in the higher multiplicity a series of noteworthy lines, including some of the most conspicuous in the visible spectrum. They are usually high-temperature lines of class III, as might be expected from their

[1] *Zeitschrift für Physik*, **39**, 122, 1926.

relatively high level of origin. The same transition, in the lower multiplicity, produces fainter lines, by no means conspicuous among the others, but important as being those which are primarily concerned in the determination of the ionization potential. The similar transition $d^{n-1}p-d^{n-1}\cdot s$ gives lines in the deep red or infra red, which are also of importance in finding the ionization potential. The 4p − 4d jump ($d^{n-2}sp-d^{n-2}s\cdot d$) gives strong multiplets, which are doubtless present in the spectra in which they have not yet been detected. Numerous iron lines, some of them of intensity as high as 25, occur in the region from λ 3300 to λ 3800, which arise from combinations between the $^7P^7D'^7F$ triad and a set of levels, not yet assorted into terms, which evidently belong to the pentad which is to be anticipated. The transition $d^{n-2}sp-d^{n-2}p^2$, which gives the well-known triplet PP′ group in calcium near λ 4300, is also presumably represented in all the spectra by lines identifiable upon close analysis.

In the spark spectra, the lines shift toward the violet in all the sequences. For *Mn* and the following elements the strongest lines, belonging to the sequence $d^{n-2}s-d^{n-2}p$, pass into the region inaccessible to the astrophysicist, though all can readily be reached in the laboratory. The sequence $d^{n-1}-d^{n-2}p$ has a discontinuity in *Mn* similar to those already described. The high-excitation lines $d^{n-2}p-d^{n-2}\cdot s$ and $d^{n-2}p-d^{n-2}\cdot d$ are, in the spark spectra, of nearly the same wave-lengths as the easily excited lines $d^{n-2}s-d^{n-2}p$. Practically all the enhanced lines of these elements (except *Ca* and *Sc*) which are ordinarily observed in the stars arise from transitions between terms not given in Tables II and IV. These terms arise from the same configurations—$d^{n-2}s$ and d^{n-1}, but are metastable and lie at higher levels than those listed, so that the energy differences between them and the lower terms of origin $d^{n-1}p$ are small enough to put the lines in the observable region. Toward the end of the sequence, beyond *Fe*, even these lines shift, for the most part, out of reach, and the spark spectra are of little astrophysical importance.

7. THE MUTUAL RELATIONS OF THE DIFFERENT SPECTRA

In conclusion, reference may be made to a curious dual resemblance between parts of any given arc spectrum in the iron group

and parts of two others. For example, it has long been familiar that a set of doublet series occurs in copper, very similar to those in potassium, and that series of singlets and triplets appear in zinc, closely resembling similar series in calcium. But in neither case does the likeness extend to the whole spectrum. Copper, for example, possesses another extensive system of doublets, with lowest term ^2D, and quartets, with the lowest terms ^4P, $^4D'$, ^4F. There is nothing at all like these in the potassium spectrum, but they may be very closely matched in that of scandium. Similarly, the calcium spectrum contains low ^3D and ^1D terms not found in zinc, and these combine with higher triads of PD'F terms, giving the system of "displaced" series, with the ^2D term of *Ca* II for limit. These terms can be matched with similar terms in nickel.

The reason for this is at once apparent on consulting the tables. The configurations d^x and d^{10-x} give exactly the same spectral terms —the main difference being that when the exponent is greater than 5 the terms are inverted and have much wider separations. It follows that in any spectrum the configuration $d^{n-2}\,s^2$, $d^{n-2}\,s\,p$, etc., may be closely matched by configurations $d^{n'-2}\,s^2$, etc., in another spectrum, if $n-2+n'-2=10$ or $n'=14-n$. Similarly the configurations $d^{n-1}\,s$, etc., may be matched if $n'=12-n$. This relation may be illustrated by writing the symbols for the elements as follows:

K Ca Sc Ti V Cr Mn
Zn Cu Ni Co Fe Mn Cr

The spectrum of any element in either row is related in structure to those of the elements in the other row and one step to the right or the left. A large portion of any one spectrum may be matched, line for line, with a similar portion of one of the related spectra, and another portion with a portion of the other. This correspondence extends beyond the terms and lines which have been listed in the tables to all the others which arise from the electronic configurations under consideration. Since, however, the terms are "regular" and of small separations for the first row, and inverted and of wide separation in the second, the spectra, even if reduced to the portions of essentially similar structure, would be somewhat dissimilar in appearance. At the end of the list, however, *Cu* and *Zn* show a "regu-

lar" multiplet separation, and the likeness to *K* and *Ca* is very conspicuous.

Two portions of spectra, consisting of septets, quintets, etc., in *Cr*, and octets, sextets, etc., in *Mn*, and including the strongest lines of each spectrum, correspond to themselves in the scheme and are unique. In these, too, series are conspicuous, as they are in *K*, *Ca*, *Cu*, and *Zn*. The reason for this is simple. These portions of the respective spectra, and these only, have for limits S terms of the spark spectrum. Under these conditions the triads and pentads of the excited states are reduced to isolated P and D terms, and the energy which would otherwise go into many multiplets is concentrated into one. Moreover, the various components of the terms go to a single limit, and the higher series members have narrow separations, which again makes the multiplets more conspicuous.

Series have been recognized, however, in all the other spectra, and, except in *V*, in both the principal parts of the spectrum.

Most of the spectra have many lines which do not belong to either of the portions already discussed—for example, those corresponding to the transitions $d^{n-2}s^2-d^{n-1}p$ and $d^{n-1}s-d^{n-2}sp$. These are the groups for which the progression in wave-length is broken by a discontinuity. They have no analogues in the spectra of any other element in the group, so that each spectrum, taken as a whole, has a definite individuality.

Among the spark spectra, the relations are somewhat simpler. The transitions $d^{n-2}s-d^{n-2}p$, etc., which give the strongest lines, produce portions of the spectrum which may be simply matched in pairs:

$$Ca^+ \quad Sc^+ \quad Ti^+ \quad V^+ \quad Cr^+ \quad Mn^+$$
$$Zn^+ \quad Cu^+ \quad Ni^+ \quad Co^+ \quad Fe^+ \quad Mn^+$$

each spectrum resembling that which is tabulated below or above it. The other portions of the spectra arising from the transitions $d^{n-1}-d^{n-2}p$ have no analogues.

The question of series and ionization potentials in these spectra, which is naturally associated with the matters here discussed, is taken up in the following paper.[1]

CARNEGIE INSTITUTION OF WASHINGTON
MOUNT WILSON OBSERVATORY
June 15, 1927

[1] *Mt. Wilson Contr.*, No. 342; *Astrophysical Journal*, **66**, 1927.

ORBIT OF THE SPECTROSCOPIC BINARY 6 π SCORPII

By O. STRUVE and C. T. ELVEY

ABSTRACT

The *orbital elements* of this *spectroscopic binary* were derived from 48 spectrograms obtained at the Yerkes and Dearborn observatories. The *spectra of both components* have been measured. $P=1.571$ day; $\gamma=-3$ km/sec.; $e=0.05$: $K_1=138$ km/sec.; $K_2=180$ km/sec.; $\omega=90°$; $T=1927$ June 15.523 U.T.; $m_2/m_1=0.77$; $(m_1+m_2)\sin^3 i=5.2\odot$; $a_1 \sin i=3{,}000{,}000$ km.

Announcement of the binary character of 6 π Scorpii was made by E. C. Pickering[1] in 1899. While examining objective-prism plates, Miss A. J. Cannon discovered that the absorption lines of this star were double. This fact was later confirmed by Professor Bailey, who also determined the period as $1^d.571$. A more detailed description of the spectrum was given by Miss Cannon in 1901.[2] However, no orbit of this star is included in Moore's "Third Catalogue of Spectroscopic Binaries,"[3] and we are not aware that any has been published.

The position of 6 π Scorpii (Boss 4062 = Co.D. 11228 = H.D. 143018) for 1900 is $\alpha\ 15^h52^m.8$; $\delta-25°50'$. According to the *Henry Draper Catalogue*, its spectral type is B_2 and its photometric magnitude is 3.00. The spectral lines are very broad and hazy and are difficult to measure. The helium lines 4026, 4388, and 4472 were usually measured in addition to the hydrogen lines $H\delta$, $H\gamma$, and $H\beta$. Occasionally it was possible to measure *Mg* 4481. Both spectral components are visible when the separation is large, but on some of the plates the fainter component was too elusive to be measured. The spectral type is the same for both components. The calcium line *K*, while probably stationary, was too faint for measurement.

Our orbit is based on 48 spectograms, of which 25 were obtained with the one-prism Bruce spectrograph of the Yerkes Observatory, giving a linear dispersion of 30 A per millimeter at λ 4500; 23 plates

[1] *Fifty-fourth Annual Report of the Director of the Astronomical Observatory of Harvard College for 1899*, p. 7.

[2] *Annals of Harvard College Observatory*, **38**, 178, Remark 46, 1901.

[3] *Lick Observatory Bulletin*, No. 355, 1924.

were secured by Elvey with the one-prism spectrograph of the Dearborn Observatory, Evanston, Illinois. A description of this instrument, designed by Professor Fox, will be given elsewhere. Its linear dispersion at λ 4340 is 39 A per millimeter. The measures of the Yerkes plates were made by Struve; the Dearborn plates were measured by Elvey. The assumed wave-lengths of the star-lines

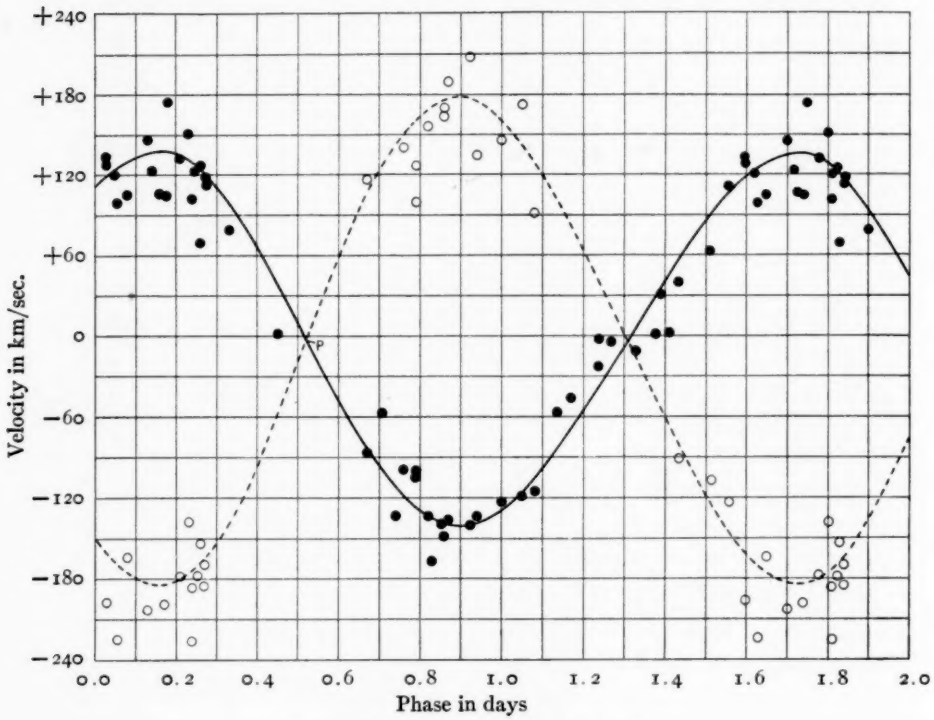

FIG. 1.—Velocity curve of 6π Scorpii

were the same for both sets of measures, and were identical with those previously used at Yerkes Observatory.[1]

Table I contains the results of the measurements. The phases were computed by means of the period found at Harvard. A plot of all observations showed that this value was sufficiently accurate to represent all our observations. Unfortunately the only old plates at our disposal were six spectrograms obtained at the Yerkes Observa-

[1] *Astrophysical Journal*, **64**, 6, 1926.

TABLE I

RADIAL VELOCITIES OF 6 π SCORPII

Date, U.T.	Observer	Observatory	Qual.	Vel. I	Vel. II	Phase
1927 Apr. 20.367	σ, S	Yerkes	g	−141.0	+208.2	0.923
Apr. 30.303	σ, H, S	Yerkes	g	+ 40.6	− 91.6	1.433
Apr. 30.381	σ, H, S	Yerkes	g	+ 63.7	−107.6	1.511
May 4.292	σ, H, S	Yerkes	g	− 57.5	.....	0.709
May 4.372	σ, H, S	Yerkes	g	−105.0	+ 98.8	.789
May 13.239	σ, H, S	Yerkes	f	+150.8	−138.3	.230
May 13.262	σ, H, S	Yerkes	g	125.1	−178.5	.253
May 13.342	σ, H, S	Yerkes	f	+ 79.4	.....	0.333
May 20.344	Elvey	Dearborn	f	−118.9	+171.1	1.051
May 27.176	σ, H, S	Yerkes	g	+333.5	−196.4	0.028
May 27.195	Elvey	Dearborn	g	119.9	.....	.047
May 27.203	σ, H, S	Yerkes	f	99.5	223.9	.055
May 27.229	σ, H, S	Yerkes	g	104.8	−163.5	.081
May 27.292	Elvey	Dearborn	g	122.6	.....	.144
May 27.309	σ, S	Yerkes	p	106.4	.....	.161
May 27.326	Elvey	Dearborn	p	+173.5	.....	.178
June 3.172	Elvey	Dearborn	g	−133.5	.....	.740
June 3.265	Elvey	Dearborn	g	166.6	.....	.833
June 3.292	Elvey	Dearborn	g	144.1	+169.1	0.860
June 8.222	Elvey	Dearborn	p	−116.6	+ 90.9	1.077
June 15.171	σ, S	Yerkes	g	+114.8	−198.7	0.171
June 15.239	σ, H, S	Yerkes	f	120.3	186.5	.239
June 15.240	Elvey	Dearborn	g	101.5	−225.3	.240
June 15.261	σ, H, S	Yerkes	g	+ 69.5	153.0	.261
June 15.272	Elvey	Dearborn	g	116.2	−184.9	.272
June 20.167	σ, H, S	Yerkes	g	+ 1.2	.....	.454
June 22.154	Elvey	Dearborn	g	−137.3	+189.5	.870
June 22.226	Elvey	Dearborn	g	144.0	133.7	0.942
June 24.093	σ, H, S	Yerkes	g	2.3	.....	1.238
June 24.166	σ, H, S	Yerkes	g	− 11.5	.....	1.311
June 24.240	Elvey	Dearborn	g	+ 1.5	.....	1.385
June 24.247	σ, H, S	Yerkes	f	30.8	.....	1.392
June 24.267	Elvey	Dearborn	f	+ 2.1	.....	1.412
June 25.099	M, S	Yerkes	g	− 87.1	116.1	0.673
June 25.183	M, S	Yerkes	f	98.8	139.6	.757
June 25.215	M, S	Yerkes	f	−110.4	+120.6	.789
June 26.127	Elvey	Dearborn	f	+145.8	−202.5	.130
June 26.205	Elvey	Dearborn	g	132.2	177.3	.208
June 26.264	Elvey	Dearborn	g	+113.9	169.1	0.267
June 27.122	Elvey	Dearborn	f	− 55.2	.....	1.125
June 27.158	Elvey	Dearborn	g	46.4	.....	1.161
June 27.233	Elvey	Dearborn	g	23.3	.....	1.236
June 27.267	Elvey	Dearborn	f	− 4.5	.....	1.270
June 29.125	Elvey	Dearborn	p	+111.0	−123.3	1.557
June 29.167	Elvey	Dearborn	g	+128.4	.....	0.028
June 30.144	σ, H, S	Yerkes	g	−123.0	+145.0	1.005
July 3.103	σ, S	Yerkes	g	134.5	155.9	0.822
July 3.143	σ, S	Yerkes	g	−139.2	+163.7	0.862

The names of the observers and the quality of the plates are designated as follows: H = C. Hujer; M = W. W. Morgan; S = F. R. Sullivan; σ = O. Struve; g = good; f = fair; p = poor.

tory in 1902,[1] and one taken in 1923. This material was not sufficient to improve the value of the period, because an error of 1 unit in the third place would produce a reversal of phase in 3.5 years. It will probably be desirable to obtain additional observations after a few years, in order to get a more accurate value of the period.

The orbital elements were obtained by the method of Lehmann-Filhés and were later improved by trial. They are collected in Table II. Since the precision of our measurements is necessarily very low, and since, furthermore, an effect of blending is readily noticeable in

TABLE II

ORBITAL ELEMENTS OF 6 π SCORPII

Element		
Velocity of system	γ	-3.0 km/sec.
Period	P	$1^d.571$
Time of periastron	T	1927 June 15.523 U.T.
Longitude of periastron	ω	90°
Eccentricity	e	0.05
Semi-amplitude I	K_1	138 km/sec.
Semi-amplitude II	K_2	180 km/sec.
Semi-major axis	$a_1 \sin i$	3,000,000 km
Minimum mass	$(m_1+m_2) \sin^3 i$	5.2 $\odot$
Mass-ratio	m_2/m_1	0.77

practically all measures where the separation of the two components is less than 150 km/sec., we have not attempted to improve the results by the method of least squares. There seems to be no constant systematic difference between Dearborn and Yerkes plates. However, there is a slight indication that the Dearborn plates give a little larger range. This may be due to a difference in interpretation, by the two measurers, of the wide, diffuse, and perhaps not quite symmetrical lines.

In determining the orbit we have considered chiefly the measurements of the stronger component. However, the fainter component yields valuable information concerning the mass-ratio of the system. The difference in the values of K is quite marked, and m_2/m_1 comes out as 0.77.

The period of 6 π Scorpii is among the shortest known for any

[1] *Ibid.*, p. 60, Star 241, 1924.

really double star of spectral type B. It is almost certain that the two components are very close together, and the unusual width of the absorption lines is probably due to axial rotation of the two components, in a period equal to that of the orbital motion.

Although it was not possible to improve the period by means of the observations of 1902, we have computed their phases from an independent zero-point and have constructed a velocity curve similar to that in Figure 1. The shape of the curve and the velocity of the system seem to be about the same as those derived from the 1927 observations, but the material is too scanty to prove definitely that no changes in the elements have taken place.

The velocity curve, together with the individual observations, is shown in the figure. Zero phase corresponds to 1927 June 15.000 U. T. (J.D. 2425047.000 U. T., the decimal fraction of the day here being given in the new G.C.T.). The velocities of the stronger component are represented by dots, while those of the fainter component are indicated by circles. The letter *P* denotes the time of periastron passage.

YERKES OBSERVATORY
DEARBORN OBSERVATORY
July 14, 1927

REVIEWS

El Firmamento. By Luis Rodés, S. J. Barcelona: Salvat Editores, S. A., 1927. 8vo. Pp. iv+586. Plates, 33; figs., 315. Price, 64 pesetas.

The director of the Observatorio del Ebro has produced a de luxe edition of an authoritative popular astronomy for the educated Spanish and Spanish-American layman.

The first part, "The Solar System," undertakes to give more than is usually expected from a similar book on the "splendor of the heavens." The inclusion of lavishly illustrated articles on meteorology, geology, physical geography would justify the change of the title of the book to *El Cosmos*, in the original sense of the word.

The second part, "The Stellar Universe," gives, in two hundred pages, a clear and accurate account of the more important methods and results of stellar research.

The usefulness of the book for reference purposes is increased by numerous synoptic tables, carefully compiled indexes according to authors (7 pages), and subjects (19 pages), and bibliographical footnotes.

Amateur photometrists will appreciate the excellent reproduction of the north polar sequence on page 213 and the corresponding table on page 556.

The book contains the same amount of useful and accurate information as do many recent college textbooks. The general reader will be attracted by the profusion of artistically reproduced photographs, by the literary style of the author, and, probably, by the modest mathematical equipment required for enjoying this book.

Of the 33 plates, the double-page Arequipa photographs of the region of η Carinae and of the Small Magellanic Cloud deserve special mention. Most of the plates are beautiful samples of American celestial and terrestrial photography. Some of the reproductions in the text, e.g., Figures 277, 338, 339, are unsatisfactory, in spite of the heavy gloss paper on which the book is printed.

In spite of careful proofreading a few dozen misprints occur. They are, however, of little importance.

Readers familiar with French or Italian, but not with Spanish, will probably be able to understand at least the technical, if not the literary, parts of the book.

Alexander Pogo

PREPARATION OF ABSTRACTS

Every article in the *Astrophysical Journal*, however short, is to be preceded by an abstract which should be submitted by the author with the manuscript. In order that the abstract may aid the reader by furnishing an index and brief summary of the contents of the article, and may also be suitable for reprinting in an abstract journal, it should be of the type of those which have been appearing in the *Astrophysical Journal* since 1920. It is requested that the abstracts be prepared in accordance with the following:

DIRECTIONS AND RULES

1. *Notes.*—Read the article carefully, taking rough notes covering all the new information reported, keeping a specially sharp lookout for new incidental results and suggestions not directly related to the main subject.

Material not new need not be described; a valuable summary of previous work, however, should be noted.

2. *Subtitles.*—Write, first, a title describing the group of results forming the main contribution of the article, including all that belong together. If there are in addition results which do not come under that title, gather them into as few groups as possible and formulate a complete and precise title for each. For examples of such subtitles see the italicized parts of the abstracts for 1920.

Each subtitle should describe the corresponding information so precisely that the chance of any investigator's being misled into thinking the article contains the particular information he desires when it does not, or vice versa, may be small. "Zeeman effect for metallic furnace spectra" is too broad unless all metals have been studied, for an investigator may be interested at the time in only one metal; but "Infra-red arc spectrum of iron to 3μ" evidently satisfies this rule.

In general a subtitle is sufficiently precise if it carries the classification of the information three stages or the equivalent, for instance if it gives (*a*) the elements and substances, (*b*) the property, and (*c*) the phase or range studied.

The subtitles should together form a complete index of the new information; that is, they should include every measurement, observation, method, suggestion, and theory which is presented as new and of value in itself. They should be complete in themselves and independent of the main title of the article.

3. *Text.*—Write a paragraph summarizing the main group of results and including the corresponding subtitle either all at the beginning or with parts scattered through the text; and then do likewise for the other groups.

A separate paragraph should be used for each distinct subject involved, but no more than necessary. All material which can easily be grouped together under a single title should be summarized in the same paragraph. Parts of

subtitles may be scattered through the text, but the subject of each paragraph must be given at the beginning.

The text should summarize the author's conclusions and should transcribe all numerical results of general interest, including all that might be looked for in a table of astronomical and physical constants, with an indication of the accuracy of each. It should give all the information that anyone not a specialist in the particular field involved might care to have in his notebook.

Complete sentences should be used except in the case of subtitles. The abstract should be made as readable as the necessary brevity will permit. Italicize subtitles but no other words or phrases.

4. *Final checking.*—Re-read the article so as to check the abstract and correct any omissions and mistakes; read the subtitles by themselves to see that they properly index the information; and read the abstract to see whether it cannot be condensed and its English be improved.

As heretofore, authors are notified that their articles cannot be accepted unless accompanied by adequate abstracts, and if articles are sent without abstracts, otherwise acceptable for publication, they will not be forwarded to the printer for composition until the abstracts are received.